

Advanced safety filter based on SOS Control Barrier and Lyapunov Functions

Michael Schneeberger, Silvia Mastellone, Florian Dörfler

Abstract—This paper presents a novel safety filter framework based on Control Barrier Functions (CBFs) and Control Lyapunov-like Functions (CLFs). The CBF guarantees forward invariance of the safe set, constraining system trajectories within state constraints, while the CLF guides the system away from unsafe states towards a nominal region, preserving the performance of a nominal controller. The first part of this work focuses on determining compatible CBF and CLF in the presence of linear or quadratic input constraints. This is achieved by formulating the CBF and CLF conditions, along with the input constraints, as Sum of Squares (SOS) constraints using Putinar’s Positivstellensatz. For solving the resulting SOS optimization problem, we employ an alternating algorithm that simultaneously searches for a feasible controller in the class of rational functions of the state. The second part of this work details the implementation of the safety filter as a Quadratically Constrained Quadratic Program (QCQP), whose constraints encode the CBF and CLF conditions as well as the input constraints. To avoid the chattering effect and guarantee the uniqueness and Lipschitz continuity of solutions, the state-dependent inequality constraints of the QCQP are selected to be sufficiently regular. Finally, we demonstrate the method on a detailed case study involving the control of a three-phase ac/dc power converter connected to an infinite bus.

I. INTRODUCTION

In various engineering applications, it is of much interest to endow a well-performant controller with safety guarantees by minimally changing its control action. This concept is commonly referred to as a *safety filter*, and a comprehensive overview of the subject can be found in [1]. An illustrative example is a finely-tuned control design based on linearization, which must be extended to adhere to hard state constraints in the nonlinear closed-loop system. We refer to such a well-performant controller as the *nominal controller*. A popular type of safety filters relies on solving a Quadratic Program (QP) at every state using a Control Barrier Function (CBF). By continuously solving the QP, the control action of the nominal controller is smoothly adjusted as the system approaches the boundary of the safe set. However, the available framework does not define the extent to which the safety filter is allowed to alter the nominal control action. This can be problematic, as the safety filter might inadvertently undermine the desired behavior of the nominal controller. Further, the main challenges in deploying such a safety filter lies in finding a viable CBF candidate and adhering to input constraints.

Michael Schneeberger and Silvia Mastellone are with the Institute of Electrical Engineering, FHNW, Windisch, Switzerland (e-mails: michael.schneeberger@fhnw.ch, silvia.mastellone@fhnw.ch), and Florian Dörfler is with the Department of Information Technology and Electrical Engineering, ETH Zürich, Switzerland, (e-mail: dorfler@control.ee.ethz.ch)

This work was supported by the Swiss National Science Foundation (SNSF) under NCCR Automation.

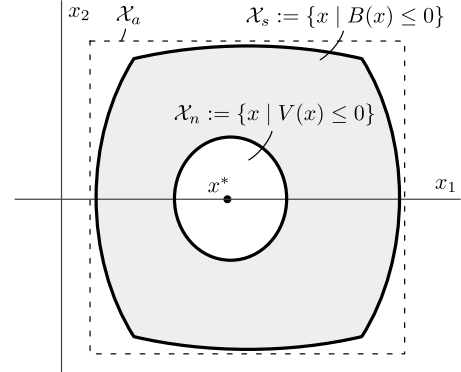


Fig. 1. (Safe set and nominal region): The safe set \mathcal{X}_s , defined as the zero sublevel set of the CBF $B(x)$, specifies the set of states for which safety can be guaranteed. The safe set must be contained within the allowable set \mathcal{X}_a , which encodes the system’s state constraints. Finally, the nominal region \mathcal{X}_n , defined as the zero sublevel set of the CLF $V(x)$, must be contained within the safe set \mathcal{X}_s .

This paper introduces an alternative framework to the safety filter concept – one that not only asserts safety but also preserves the nominal control performance. This is accomplished by delineating a *nominal region* \mathcal{X}_n , as shown in Figure 1, where the nominal control action is guaranteed to remain unchanged. This is motivated by the observation that the control performance is typically specified only within a vicinity surrounding the desired closed-loop equilibrium point. Consequently, we are left with a distinct region bounded by the system’s state constraints, where modifications of the control action are permitted in order to keep the system safe.

Our safety filter is realized based on solving a Quadratic Constraint Quadratic Program (QCQP) at every state using CBFs and Control Lyapunov-like Functions (CLFs). A QCQP instead of a simple QP is employed to encode quadratic input constraints. While the CBF represents a conventional approach for implementing a safety filter, we leverage the CLF to encode a smooth transition from the safety filter’s operation to the nominal control operation. The smooth transition is realized by imposing three conditions:

- 1) the zero-sublevel set of the CLF defines the nominal region \mathcal{X}_n ,
- 2) the CLF ensures finite-time convergence to the nominal region while guaranteeing state and input constraints,
- 3) the nominal region is chosen to ensure forward invariance of the closed-loop system under the nominal controller.

To identify viable CBF and CLF candidates as well as a solution for the QCQP at every state, we propose a Sum-of-Squares

(SOS) optimization approach. This approach seeks compatible polynomial CBF and CLF candidates that adhere to the linear and quadratic input constraints. To solve the SOS program, we deploy an alternating algorithm that simultaneously searches for a feasible controller in the class of rational functions of the state.

The concept of our safety filter resembles the integration of a CLF with a CBF to attain both safety and stabilization. Such a unification, although just with a single function, has been initially proposed in [2]. The integration of both CLF and CBF into an optimization-based controller has since become a well-established concept, see the survey in [3]. As previously noted, when utilizing an optimization-based controller, it is imperative to ensure the existence of at least one feasible solution at every state. This can be accomplished by introducing a slack variable that deactivates CLFs and CBFs based on their respective priorities, as shown in [4]. Alternatively, it is possible to compute compatible CLFs and CBFs using SOS tools. To the best of authors' knowledge, two methods exist for encoding the compatibility between CLFs and CBFs in terms of SOS constraints. In the absence of input constraints, the first method, as described in [5], introduces an SOS constraint for each CLF/CBF pair. The second method establishes compatibility by introducing a polynomial or rational state-feedback controller, as outlined in [6], [7]. Such a controller can also be used to enforce linear input constraints, as demonstrated in [8]. Another noteworthy approach for imposing input constraints using a contrapositive statement, albeit without ensuring compatibility, is introduced in [9]. These methods introduce auxiliary polynomials that make the resulting SOS problem bilinear in its decision variables. In [10], an alternating algorithm is proposed to solve this bilinear SOS problem. One challenge in seeking CLF and CBF candidates through an alternating algorithm is to identify an initial feasible point. In their work in [11], the authors constrained their search for an initial CBF to scalar functions of a specific form. This restriction allows to reformulate the problem with linearity in its decision variables.

In this paper, we expand upon the methodology of synthesizing a rational controller to find compatible CLF and multiple CBFs. The introduction of multiple CBFs provides us with greater flexibility in constructing the safe set, as demonstrated in [7]. We then introduce a novel approach for encoding quadratic input constraints on the rational controller. This ensures feasibility of the resulting QCQP-based controller, even in the case of quadratic input constraints – an issue that, to the authors' knowledge, remained unsolved. Instead of imposing the condition for each CBF separately, as pointed out in [12], we relax these conditions when the corresponding CBF is not active. Moreover, the CLF condition can also be relaxed by leveraging the forward invariance property of the CBFs, similar to [13] for autonomous systems. By using Putinar's Positivstellensatz, the resulting CBF and CLF conditions can be translated to SOS constraints. We propose an initialization procedure to find an initial feasible set of parameters. The main algorithm then iterates between searching over one set of variables while keeping the others fixed, while maximizing the volume of the safe set. To avoid the chattering effect and

guarantee the uniqueness and Lipschitz continuity of solutions, the state-dependent inequality constraints of the QCQP are selected to be sufficiently regular. Finally, we tested our framework on a detailed three-phase ac/dc converter system connected to an infinite bus. We successfully synthesized a safety filter that ensures satisfaction of the state constraints on the dc-link voltage, as well as the line current, while adhering to the quadratic input constraints. We further tracked an a priori unspecified quadrature current reference of the ac/dc converter by integrating it as a state into a slightly modified system model.

The remainder of the paper is structured as follows: In Section II, the preliminaries and notation are discussed. Section III introduces the concept of the advanced safety filter, its properties, and the resulting problem statement. In Section IV, we formulate the SOS optimization problem to identify compatible CBF and CLF candidates satisfying linear and quadratic input constraints. Section V formulates the advanced safety filter as a Lipschitz-continuous QCQP-based controller. In Section VI, we introduce an alternating algorithm designed to solve the SOS optimization problem. Numerical simulations, presented in Section VII, are provided to demonstrate the efficacy of our safety filter. Finally, Section VIII concludes the paper.

II. PRELIMINARIES & NOTATION

A. Notation

The shorthand $\mathcal{I}_t := \{1, 2, \dots, t\}$ designates a range of natural numbers from 1 to t . $R[x]$ refers to the set of scalar polynomials in variables $x \in \mathbb{R}^n$, and $\Sigma[x]$ refers to the set of scalar SOS polynomials in variables $x \in \mathbb{R}^n$. If $p(x) \in \Sigma[x]$, it can be expanded to

$$p(x) = Z(x)^T Q Z(x), \quad (1)$$

where $Z(x)$ is a vector of monomials in x , and Q is a square positive semidefinite matrix.

Throughout the paper, we consider a polynomial control system, affine in the control action $u \in \mathbb{R}^m$, and described as

$$\dot{x} = F_c(x, u) = f(x) + G(x)u, \quad (2)$$

where $x \in \mathbb{R}^n$ is the state, $f(x) \in (R[x])^n$ is a polynomial vector field, and $G(x) \in (R[x])^{n \times m}$ is a polynomial matrix. System (2) with a polynomial state feedback control policy $u_{cl}(x) \in (R[x])^m$ results in a closed-loop system of the form

$$\dot{x} = F_{cl}(x) = f(x) + G(x)u_{cl}(x). \quad (3)$$

The state x^* is called an equilibrium of the system (3), if $F_{cl}(x^*) = 0$.

The interior of a set $\mathcal{X} \subseteq \mathbb{R}^n$ is denoted by $\text{int}(\mathcal{X})$. A subset $\mathcal{X} \subseteq \mathbb{R}^n$ is called *forward invariant* (cf. [14, Theorem 4.4]) with respect to system (3) if for every $x(0) \in \mathcal{X}$, $x(t) \in \mathcal{X}$ for all $t \geq 0$. A system (3) is called *safe* (cf. [15]) w.r.t. an *allowable set* of states $\mathcal{X}_a \subseteq \mathbb{R}^n$ and the *safe set* $\mathcal{X}_s \subseteq \mathbb{R}^n$, if \mathcal{X}_s is forward invariant and $\mathcal{X}_s \subseteq \mathcal{X}_a$. We say that a controller $u_{cl}(x)$ guarantees safety if the corresponding closed-loop system is safe.

Assumption 1 (standing assumption): In the following, the allowable set \mathcal{X}_a is assumed compact and regular.

B. Putinar's Positivstellensatz

Before stating Putinar's P-satz, we need to introduce two preliminary definitions.

Definition 1: A quadratic module generated by polynomials $f_2, \dots, f_n \in R[x]$ is defined by

$$\mathbf{M}(f_2, \dots, f_n) := \left\{ \gamma_0 + \sum_{i=2}^n \gamma_i f_i \mid \gamma_0, \dots, \gamma_n \in \Sigma[x] \right\}. \quad (4)$$

Definition 2: A quadratic module $\mathbf{M}(f_2, \dots, f_n)$ is said to be *Archimedean* when there exists a polynomial $f \in \mathbf{M}(f_2, \dots, f_n)$ such that $\{x \in \mathbb{R}^n \mid f \geq 0\}$ is a compact set.

The following theorem states Putinar's P-satz (cf. [16, Theorem 3.20]).

Theorem 1: Given polynomials $f_1, \dots, f_n \in R[x]$ such that the quadratic module $\mathbf{M}(f_2, \dots, f_n)$ is Archimedean, and

$$\left\{ x \in \mathbb{R}^n \mid f_1(x) \leq 0, f_2(x) \geq 0, \dots, f_n(x) \geq 0 \right\} = \emptyset, \quad (5)$$

then

$$f_1 \in \mathbf{M}(f_2, \dots, f_n). \quad (6)$$

If the set in (5) is empty, Putinar's P-satz ensures that the polynomials $\gamma_0, \gamma_2, \dots, \gamma_n$, as defined in (4), exist without specifying their degree. To find these polynomials computationally requires to iteratively increase the degree of the polynomials until a solution can be found for (6). An increase in the degree of the polynomials will, however, deteriorate computation time. For many practical examples of interest, however, low-degree polynomials suffice.

Condition (6) can also be expressed more explicitly through the condition that there exists $\gamma_1, \gamma_2, \dots, \gamma_n \in \Sigma[x]$ such that

$$\gamma_1 f_1 - \gamma_2 f_2 - \dots - \gamma_n f_n \in \Sigma[x]. \quad (7)$$

Assuming the empty-set condition in (5) holds, a solution to (7) involving $\gamma_1(x) = 1$ is guaranteed by Putinar's P-satz to exist when the degrees of the polynomials are possibly unbounded. In this case, the introduction of the SOS polynomial $\gamma_1(x)$ needlessly increases the set of feasible polynomials $f_1(x)$. However, when the degrees of the polynomials are truncated, this assertion may no longer hold true, justifying the utilization of $\gamma_1(x)$. For the rest of the paper, we refer to both inclusions, (6) and (7), as an *SOS constraint*.

III. SPECIFICATIONS AND PROBLEM STATEMENT

A. Specifications

The concept of a *safety filter* (see Figure 2) is based on the idea of enhancing the behavior of a previously designed *nominal controller* $u_n(x)$ with safety guarantees. The nominal controller, may represent a controller that is successfully deployed in the field and should not be altered if possible. An illustrative example is a finely-tuned linear controller, which is highly performant near the equilibrium point. The safety filter adjusts the control action of the nominal controller, ideally in a minimal way, to render the system safe with respect to an allowable set \mathcal{X}_a and a safe set \mathcal{X}_s . The allowable set \mathcal{X}_a delineates the states within which the system is designed to operate. Departing from the set may lead to irreversible

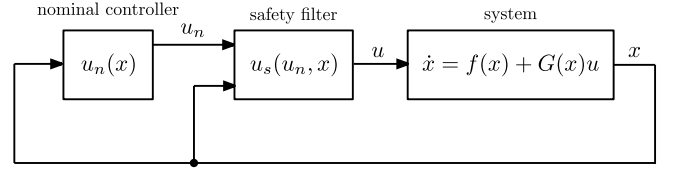


Fig. 2. (Representation of the safety filter concept): The safety filter $u_s(u_n, x)$ adjusts the nominal control action $u_n(x)$ – if necessary – to guarantee safe operation.

damage to the system. The safe set \mathcal{X}_s denotes a set of initial states from which the future trajectory will remain within it. Therefore, we require that the safe set \mathcal{X}_s is strictly contained within the allowable set \mathcal{X}_a , i.e.,

$$\mathcal{X}_s \subseteq \text{int}(\mathcal{X}_a). \quad (8)$$

The safe set is preferably chosen large in volume to closely approximate the allowable set.

The characterization of a safety filter does not specify the extent to which we are allowed to alter the nominal control action. This can be problematic, as the safety filter might inadvertently undermine the desired behavior of the nominal controller. In contrast, the *advanced safety filter* $u_s(x)$ specifies a distinct region \mathcal{X}_n , where the nominal control action remains unaffected. That is, for all $x \in \mathcal{X}_n$:

$$u_s(x) = u_n(x). \quad (9)$$

This *nominal region* \mathcal{X}_n is required to be forward invariant under the nominal control $u_n(x)$, and to be strictly contained within the safe set, i.e.,

$$\mathcal{X}_n \subseteq \text{int}(\mathcal{X}_s). \quad (10)$$

Moreover, if the nominal controller asymptotically stabilizes the system to the equilibrium point $x^* \in \mathcal{X}_n$, the advanced safety filter should preserve the stability guarantee across the entire safe set. This is already accomplished inside the nominal region due to its forward invariance property. Hence, we only need to additionally ensure a finite-time convergence to the nominal region for all trajectories originating within the *transitional region* defined as:

$$\mathcal{X}_t := \mathcal{X}_s \setminus \text{int}(\mathcal{X}_n). \quad (11)$$

B. CBF and CLF conditions formalizing the specifications

The forward invariance property of the safe set \mathcal{X}_s is asserted by a Control Barrier Function (CBF) $B(x)$ defined as the point-wise maximum of a set of continuously differentiable functions $B_i : \mathbb{R}^n \rightarrow \mathbb{R}$ indexed by \mathcal{I}_t :

$$B(x) := \max_{i \in \mathcal{I}_t} B_i(x). \quad (12)$$

The safe set is given by its zero sublevel set:

$$\mathcal{X}_s := \{x \mid B(x) \leq 0\}.$$

Assumption 2: We assume the safe set \mathcal{X}_s to be regular in the sense that $\forall x \in \mathcal{X}_s, \exists z \in \mathbb{R}^n, \forall i \in \mathcal{I}_t$ [17, Definition 4.9]:

$$B_i(x) + \nabla B_i(x)^T z < 0$$

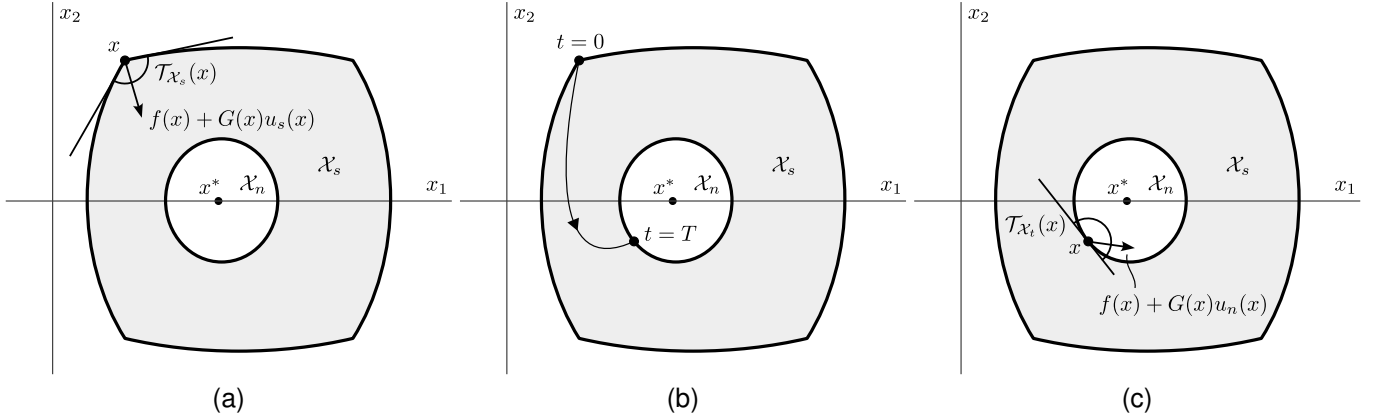


Fig. 3. (Forward invariance and finite-time convergence): The advanced safety filter is characterized by the following specifications: (a) the safe set \mathcal{X}_s is forward invariant as encoded in (13), (b) finite-time convergence towards the nominal region \mathcal{X}_n as encoded in (17), and (c) the nominal region is forward invariant under the nominal controller $u_n(x)$ as encoded in (19) assuming $d(x) = 0$.

The regularity assumption in Assumption 2 is a mild one, and it generically holds true, if $B_i(x)$ is chosen as a polynomial. It implies that the interior of the safe set is given by $\text{int}(\mathcal{X}_s) = \{x \mid B_i(x) < 0 \quad i \in \mathcal{I}_t\}$. Examples of polynomials that violate the regularity assumption can be found in [17, Chapter 4.2].

To ensure forward invariance of \mathcal{X}_s , as shown in Figure 3(a), the CBF $B(x)$ needs to satisfy Nagumo's theorem, that is, $\forall x \in \partial\mathcal{X}_s, \exists u \in \mathbb{R}^m$ (cf. [17, Nagumo's Theorem 4.7]):

$$f(x) + G(x)u \in \mathcal{T}_{\mathcal{X}_s}(x), \quad (13)$$

where $\mathcal{T}_{\mathcal{X}_s}(x)$ is the tangent cone to \mathcal{X}_s at x . Under Assumption 2, the tangent cone is defined by

$$\mathcal{T}_{\mathcal{X}_s}(x) := \{z \mid \nabla B_i(x)^T z \leq 0 \quad i \in \text{Act}(x)\}, \quad (14)$$

where $\text{Act}(x) := \{i \in \mathcal{I}_t \mid B_i(x) = 0\}$ denotes the set of active constraints. This formulation of the tangent cone will become useful in the subsequent section of the paper.

The choice of the number of continuously differentiable functions $B_i(x)$ is made to ensure a close fit of the safe set \mathcal{X}_s to the allowable set \mathcal{X}_a . Consequently, in this paper, we assume that the allowable set is defined by the same number of polynomials:

$$\mathcal{X}_a := \left\{x \mid w_i(x) \leq 0 \quad \forall i \in \mathcal{I}_t\right\}, \quad (15)$$

where $w_i \in R[x]$, $i \in \mathcal{I}_t$, whose zero-sublevel set $\{x \mid w_i(x) \leq 0\}$ is assumed to be compact. This compactness condition is important for applying Putinar's P-satz in the following section of the paper. The containment condition in (8) is inferred by the slightly stricter conditions for every $i \in \mathcal{I}_t$:

$$\{x \mid B_i(x) \leq 0\} \subseteq \{x \mid w_i(x) < 0\}. \quad (16)$$

This can be seen from $\bigcap_{i \in [\ell]} \{x \mid B_i(x) \leq 0\} \subseteq \bigcap_{i \in [\ell]} \{x \mid w_i(x) < 0\}$ implying $\mathcal{X}_s \subseteq \text{int}(\mathcal{X}_a)$.

The finite-time convergence property of the safety filter, as outlined in the specifications, is asserted by a Control Lyapunov Function (CLF) defined by a continuously differentiable function $V : \mathbb{R}^n \rightarrow \mathbb{R}$. This function needs to satisfy a

Control Lyapunov-like condition in the transitional region \mathcal{X}_t , as shown in Figure 3(b). Namely, $\forall x \in \mathcal{X}_t, \exists u \in \mathbb{R}^m$:

$$\nabla V(x)^T (f(x) + G(x)u) + d(x) \leq 0 \quad (17)$$

with *dissipation rate*

$$d(x) := \lambda(x) (V(x) + V_0) > 0, \quad (18)$$

where $\lambda : \mathbb{R}^n \rightarrow \mathbb{R}_{>0}$ is a Lipschitz continuous function, and $V_0 \leq \min_x (V(x))$ is a constant value, ensuring $d(x)$ is strictly positive (and thus $V(x)$ strictly decaying) in the transitional region \mathcal{X}_t . We define the nominal region as the zero sublevel set of $V(x)$:

$$\mathcal{X}_n := \{x \mid V(x) \leq 0\}.$$

Consequently, the transitional region is given by:

$$\mathcal{X}_t := \{x \mid B(x) \leq 0 \leq V(x)\}.$$

The next lemma establishes the finite-time convergence property associated with the CLF $V(x)$. Its proof can be found in the appendix.

Lemma 1: Given a Lipschitz-continuous controller $u_s : \mathbb{R}^n \rightarrow \mathbb{R}^m$ that satisfies condition (17) with $u := u_s(x)$ and renders the safe set \mathcal{X}_s forward invariant, then for all trajectories of system (3) starting in the safe set \mathcal{X}_s there exists some finite $T \geq 0$ such that $x(t) \in \mathcal{X}_n$ for all $t \geq T$.

Note that condition (17) also ensures forward invariance of the nominal region \mathcal{X}_n . Indeed, at the boundary of the nominal region, an input u satisfying (17) implies the containment of $f(x) + G(x)u$ in the tangent cone $\mathcal{T}_{\mathcal{X}_n}(x)$ (cf. [17, Nagumo's Theorem 4.7]). Additionally, to make the nominal region forward invariant w.r.t. the nominal controller $u_n(x)$, as depicted in Figure 3(c), we propose the condition that $\forall x \in \partial\mathcal{X}_n$:

$$\nabla V(x)^T (f(x) + G(x)u_n(x)) + d(x) \leq 0. \quad (19)$$

As we will see in Section V, by adopting a slightly stricter forward invariance condition in (19) involving the dissipation rate $d(x)$, we ensure the existence of a controller that smoothly transitions to the nominal control operation when approaching the nominal region \mathcal{X}_n , as specified in (9).

C. Problem statement

The challenge of deriving the advanced safety filter can be divided into two subproblems. The first subproblem involves finding a CBF $B(x)$ and CLF $V(x)$ that concurrently fulfill the forward invariance and finite-time convergence properties outlined in the preceding chapter. The second subproblem resolves around constructing a safe, Lipschitz-continuous controller $u_s(x)$ from the CBF $B(x)$ and CLF $V(x)$.

The first subproblem involves, among others, constructing a rational controller $u_{\text{SOS}}(x)$ to prove the compatibility of the forward invariance and finite-time convergence conditions in (13) and (17). This is a complex task that involves to simultaneously searching for a controller $u_{\text{SOS}}(x)$, and functions $B(x)$ and $V(x)$. Furthermore, we necessitate that the controller $u_{\text{SOS}}(x)$ remains within the pre-specified compact semi-algebraic set \mathcal{U} encoding linear and quadratic input constraints.

Problem 1: Given a dynamical system (3), an allowable set of states \mathcal{X}_a and a nominal controller $u_n(x) \in \mathcal{U}$, find a CBF $B(x)$ and CLF $V(x)$ such that:

- (set containment) the containment conditions in (8) and (10) are satisfied,
- (finite-time convergence) the CLF condition in (17) is satisfied,
- (forward-invariance of \mathcal{X}_s) CBF and CLF conditions in (13) and (17) are satisfied on $\partial\mathcal{X}_s$ for the same u ,
- (forward-invariance of \mathcal{X}_n) CBF condition in (19) is satisfied,
- (objective) CBF $B(x)$ maximizes the volume of the safe set, denoted by $\text{vol}(\mathcal{X}_s)$.

For the second subproblem, given a CBF $B(x)$ and a CLF $V(x)$ as described in Problem 1, a safety filter $u_s(x)$ can be realized by continuously solving a Quadratically Constrained Quadratic Program (QCQP) in closed-loop for every state $x \in \mathbb{R}^n$ along the trajectory:

$$u_s(x) := \min_{u \in \mathcal{U}} \|u_n(x) - u\|^2 \quad (20)$$

$$\text{s.t. } C(x)u + b(x) \leq 0,$$

where the input constraint set \mathcal{U} is characterized by polynomials that are either linear or quadratic in u , $C : \mathbb{R}^n \rightarrow \mathbb{R}^{(t+1) \times m}$ is a state dependent matrix, and $b : \mathbb{R}^n \rightarrow \mathbb{R}^{t+1}$ is a state dependent vector. Our objective is to define the inequality constraints of the QCQP given by $C(x)$ and $b(x)$ such that both the forward invariance and finite-time convergence conditions, as outlined in (13) and (17), are satisfied. These conditions are linear in u and can therefore be encoded as linear inequality constraints in the QCQP. Furthermore, $C(x)$ and $b(x)$ are selected sufficiently regular such that the resulting safety filter $u_s(x)$ is Lipschitz-continuous. The problem of finding an advanced safety filter can therefore be summarized as follows:

Problem 2: Given a dynamical system (3), a Lipschitz-continuous nominal controller $u_n(x)$, a CBF $B(x)$ and CLF $V(x)$, as specified in Problem 1, find functions $C(x)$ and $b(x)$ such that the resulting safety filter $u_s(x)$ in (20) is feasible for all $x \in \mathbb{R}^n$, satisfies the forward invariance and finite-time convergence conditions (13) and (17) with $u := u_s(x)$,

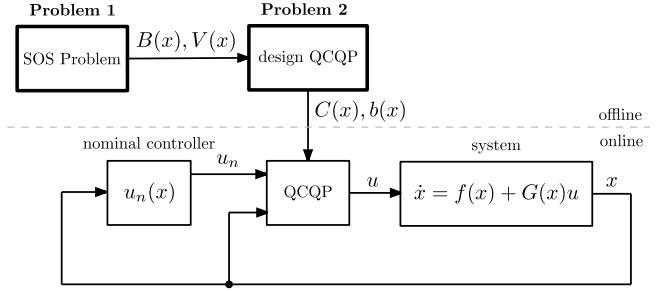


Fig. 4. (Representation of the 2-step approach for formulating the safety filter): Problem 1 involves searching for compatible CBF $B(x)$ and CLF $V(x)$, while Problem 2 involves defining the linear inequalities of the QCQP.

coincides with the nominal controller on \mathcal{X}_n , as described in (9), and is Lipschitz-continuous.

In Section IV, we delve into a solution for Problem 1, while a solution for Problem 2 is derived in Section V.

IV. CONSTRUCTING CBF AND CLF USING SOS OPTIMIZATION

A. SOS formulation of CBF and CLF conditions

The objective of this subsection is to derive sufficient SOS conditions that encode the forward invariance condition on \mathcal{X}_s and \mathcal{X}_n , as specified in (13) and (19), and the finite-time convergence condition, as specified in (17). We further demonstrate that these sufficient SOS conditions are not overly conservative and pose no practical concerns.

The forward invariance condition in (13) involves the set of active constraints $\text{Act}(x)$, a construction that cannot be directly expressed as an SOS constraint. To address this issue, we first consider the polynomials $B_i(x)$, $i \in \mathcal{I}_t$, defining the CBF $B(x)$ in (12), as independent CBFs in their own right. By ensuring compatibility among these CBFs $B_i(x)$ as proposed in [7], we demonstrate in Lemma 2 the sufficiency of the resulting SOS constraints with respect to forward invariance condition in (13) (involving the desired CBF $B(x)$). The CBF condition for each $B_i(x)$, $i \in \mathcal{I}_t$, is expressed as $\forall x \in \{x \in \mathcal{X}_s \mid B_i(x) = 0\}, \exists u \in \mathbb{R}^m$:

$$\nabla B_i(x)^T (f(x) + G(x)u) \leq 0. \quad (21)$$

Another challenge in converting conditions (21) and (17) to SOS constraints is the presence of the existential quantifier $\exists u \in \mathbb{R}^m$. However, following the approach in [10], we can reformulate these conditions without the need for an existential quantifier. The CBF condition (21) can be expressed as $\forall x \in \{x \in \mathcal{X}_s \mid B_i(x) = 0, \nabla B_i(x)^T G(x) = 0\}$:

$$\nabla B_i(x)^T f(x) \leq 0. \quad (22)$$

Similarly, the finite-time convergence condition in (17) can be formulated as $\forall x \in \{x \in \mathcal{X}_t \mid \nabla V(x)^T G(x) = 0\}$:

$$\nabla V(x)^T f(x) + d(x) \leq 0. \quad (23)$$

In order to render the problem tractable, we restrict our attention to polynomial candidates $B_i \in R[x]$, $i \in \mathcal{I}_t$, and

polynomial candidate $V \in R[x]$. We then apply Putinar's P-satz, as stated in Theorem 1, on a slightly more stringent conditions compared to (22), (23) and (19), where the inequality is replaced by a strict inequality. These more stringent conditions are summarized as the following empty-set conditions, $i \in \mathcal{I}_t$:

$$\{x \mid -\nabla B_i(x)^T f(x) \leq 0, \nabla B_i(x)^T G(x) = 0, B_i(x) = 0, -B_{\mathcal{I}_t}(x) \geq 0\} = \emptyset \quad (24a)$$

$$\{x \mid -\nabla V(x)^T f(x) - d(x) \leq 0, \nabla V(x)^T G(x) = 0, V(x) \geq 0, -B_{\mathcal{I}_t}(x) \geq 0\} = \emptyset \quad (24b)$$

$$\{x \mid \nabla V(x)^T (f(x) + G(x)u_n(x)) + d(x) \leq 0, V(x) = 0\} = \emptyset, \quad (24c)$$

where $B_{\mathcal{I}_t}(x) = [B_1(x) \ \dots \ B_t(x)]^T$ is a vector of CBFs. The resulting SOS constraints are summarized below. A detailed derivation of the SOS constraint (25) from the empty-set condition (24) is given in Section IX-B. For clarity, we omit the brackets and variables in the function notation.

$$-\nabla B_i^T (s_i f + G p_i) \in \mathbf{M}(B_i, -B_{\mathcal{I}_t}) \quad (25a)$$

$$-\nabla V^T (s_0 f + G p_0) - s_0 d \in \mathbf{M}(V, -B_{\mathcal{I}_t}) \quad (25b)$$

$$-\nabla V^T (f + G u_n) - d \in \mathbf{M}(V, -V), \quad (25c)$$

for some $p_i \in (R[x])^m$ and $s_i \in \Sigma[x]$, $i \in \{0\} \cup \mathcal{I}_t$. To achieve the simultaneous satisfaction of forward invariance and finite-time convergence conditions (13) and (17) on the boundary of the safe set $\partial \mathcal{X}_s$, as specified in Problem 1, we equate the polynomials $p_i(x)$ and $s_i(x)$, $i \in \{0\} \cup \mathcal{I}_t$. The resulting SOS constraints are given as:

$$-\nabla B_i^T (s f + G p) \in \mathbf{M}(B_i, -B_{\mathcal{I}_t}) \quad (26a)$$

$$-\nabla V^T (s f + G p) - s d \in \mathbf{M}(V, -B_{\mathcal{I}_t}) \quad (26b)$$

$$-\nabla V^T (f + G u_n) - d \in \mathbf{M}(V, -V), \quad (26c)$$

for $i \in \mathcal{I}_t$, and some $p \in (R[x])^m$, and $s \in \Sigma[x]$.

Remark 1: The polynomials $p(x)$ and $s(x)$ induce (after dividing (26a) and (26b) by $s(x)$) a rational controller $u_{\text{SOS}}(x) := p(x)/s(x)$, employed to prove compatibility of the CBFs $B_i(x)$ and CLF $V(x)$.

The proof of Lemma 2 can be found in the appendix.

Lemma 2: If $s(x) > 0$ and Assumption 2 is satisfied, then the SOS constraints in (26) are sufficient conditions for the forward invariance and finite-time convergence property in (17), (13) and (19) to hold simultaneously with $u := p(x)/s(x)$.

The SOS constraints in (26) imply the inequalities:

$$\nabla B_i^T (s f + G p) + \gamma_{0,i} B_i - \gamma_{1,i}^T B_{\mathcal{I}_t} \leq 0 \quad (27a)$$

$$\nabla V^T (s f + G p) + s d + \gamma_{0,0} V - \gamma_{1,0}^T B_{\mathcal{I}_t} \leq 0 \quad (27b)$$

$$\nabla V^T (f + G u_n) + d + \gamma_n V \leq 0, \quad (27c)$$

for some $\gamma_{0,i}, \gamma_n \in R[x]$, $p \in (R[x])^m$, $s, \gamma_{0,0} \in \Sigma[x]$, and $\gamma_{1,i}, \gamma_{1,0} \in (\Sigma[x])^t$, $i \in \mathcal{I}_t$.

Lemma 2 only provides sufficient conditions as a consequence of Putinar's P-satz. However, adding an arbitrary small perturbation $\epsilon > 0$ to the SOS constraints in (26) results in inequalities, as specified in (27), where the inequality is replaced by a strict inequality. These more stringent inequalities imply

the desired conditions (13), (17) and (19) from Lemma 2, establishing the SOS constraints (involving an arbitrary small ϵ) as necessary conditions. Hence, for all practical intents and purposes, the solution set of the SOS constraints in (26) encompasses the desired set of CBFs and CLFs.

B. SOS formulation of input constraints

In the following, we consider two types of inputs constraints: linear and quadratic input constraints. Consider the linear input constraint set

$$\mathcal{U} = \{u \mid Au \leq b\}, \quad (28)$$

where $A \in \mathbb{R}^{m \times l}$ and $b \in \mathbb{R}^l$. These linear input constraints can be encoded by the SOS constraints:

$$-a_i p(x) + b_i s(x) \in \mathbf{M}(-B_{\mathcal{I}_t}), \quad (29)$$

where a_i is the i th row of A , $i \in \mathcal{I}_l$, and $p(x)$ and $s(x)$ are as in (26). Next, we consider the quadratic input constraint

$$\mathcal{U} = \{u \mid (u - u_0)^T Q_u (u - u_0) \leq u_{\max}^2\}, \quad (30)$$

for some $Q_u \succeq 0$ and $u_0 \in \mathbb{R}^m$. The quadratic input constraint (30) can be encoded using the SOS constraint involving variables $x \in \mathbb{R}^n$ and $v \in \mathbb{R}^m$:

$$-v^T Q_u (p(x) - s(x)u_0) + s(x)u_{\max}^2 \in \mathbf{M}(-f_u, -B_{\mathcal{I}_t}), \quad (31)$$

where $f_u(x, v) := v^T Q_u v - u_{\max}^2 \in R[x, v]$ encodes the input constraint set in (30). The following lemma establishes the implication of the input constraints based on the SOS constraints. The proof is reported in the appendix.

Lemma 3: If $s(x) > 0$, a solution $p(x)$ and $s(x)$ to the SOS constraint (29), resp. (31), also satisfies the input constraints (28), resp. (30), with $p(x)/s(x) \in \mathcal{U}$ for all $x \in \mathcal{X}_s$.

C. Safe set and nominal region requirement

In this section, we express the containment conditions of the allowable set \mathcal{X}_a , the safe set \mathcal{X}_s and the nominal region \mathcal{X}_n (as illustrated in Figure 1) in terms of SOS constraints. The containment condition of \mathcal{X}_s inside \mathcal{X}_a , as defined in (16), can be expressed as the empty-set condition for all $i \in \mathcal{I}_t$:

$$\{x \mid B_i(x) \leq 0, w_i(x) \geq 0\} = \emptyset. \quad (32)$$

Using Putinar's P-satz in Theorem 1, we translate (32) into the SOS constraints for all $i \in \mathcal{I}_t$:

$$B_i \in \mathbf{M}(w_i). \quad (33)$$

Similarly, the containment condition of \mathcal{X}_n inside \mathcal{X}_s in (10), can be expressed as the empty-set condition for all $i \in \mathcal{I}_t$:

$$\{x \mid V(x) \leq 0, B_i(x) \geq 0\} = \emptyset. \quad (34)$$

Using Putinar's P-satz, we translate (34) into the SOS constraints for all $i \in \mathcal{I}_t$:

$$-B_i \in \mathbf{M}(V) \in \Sigma[x]. \quad (35)$$

D. Resulting SOS problem

The solution to Problem 1, i.e., finding suitable functions $B_i(x)$, $i \in \mathcal{I}_t$, and $V(x)$ can be obtained by solving the following SOS optimization problem:

$$\begin{aligned} & \text{find} && V, B_i, p \in (\mathbb{R}[x])^m, s \in \Sigma[x], \\ & \text{maximize} && \text{vol}(\mathcal{X}_s) \\ & \text{subject to} && (26), (29), (31), (33) \text{ and } (35) \\ & && s - \epsilon \in \Sigma[x], \end{aligned} \quad (36)$$

where (26) encode the forward invariance and finite-time convergence property, (29) and (31) encode linear and quadratic input constraints, (33) and (35) encode the set containment properties, and a constant $\epsilon > 0$ assures that $s(x) > 0$.

V. SAFETY FILTER IMPLEMENTATION

The objective of this section is to implement the safety filter to achieve a smooth transition from the safety filter operation to the nominal control operation. Given a linear and quadratic input constraints set \mathcal{U} , we propose the following realization of the QCQP in (20), where the linear constraints are designed to encode the CLF and CBF conditions:

$$C(x) := \begin{bmatrix} \nabla V(x)^T G(x) \\ \nabla B_1(x)^T G(x) \\ \vdots \\ \nabla B_t(x)^T G(x) \end{bmatrix} \quad (37a)$$

$$b(x) := \begin{bmatrix} \nabla V(x)^T f(x) + d(x) \\ \nabla B_1(x)^T f(x) \\ \vdots \\ \nabla B_t(x)^T f(x) \end{bmatrix} - \begin{bmatrix} r_0(x) \\ r_1(x) \\ \vdots \\ r_t(x) \end{bmatrix}. \quad (37b)$$

Here $r_i : \mathbb{R}^n \rightarrow \mathbb{R}$, $i \in \{0\} \cup \mathcal{I}_t$, are slack variables with $r_0(x)$ encoding the allowed reduction of the dissipation rate, and $r_i(x)$, $i \in \mathcal{I}_t$, encoding the allowed 'safety violation', using the terminology of [18]. To give a preview on the design trade-offs: By selecting a larger positive value for $r_i(x)$, $i \in \mathcal{I}_t$, within the safe set \mathcal{X}_s allows for larger positive values of $\dot{B}(x) = \nabla B(x)^T \dot{x}$. This renders the safety filter more passive within $\text{int}(\mathcal{X}_s)$, and thus leaves more room to satisfy the CLF constraint. However, an overly large value for $r_i(x)$, $i \in \mathcal{I}_t$, can result in abrupt modifications of the control action when approaching the boundary of the safe set. An informal discussion of $r_0(x)$ can be found in Example 1.

To ensure a smooth transition from the safety filter operation to the nominal control operation, the function $r_i(x)$ are selected to be twice differentiable and satisfy the following conditions:

- 1) the forward invariance and finite-time convergence conditions specified in (13) and (17) are satisfied with input $u := u_s(x)$,
- 2) the QCQP (20) remains feasible for all $x \in \mathbb{R}^n$, and
- 3) the nominal control action is preserved on the set \mathcal{X}_n , as specified in (9).

The first condition translates to upper bounds $r_i^+(x)$ on $r_i(x)$, while the second and third conditions translate to lower bounds $r_i^-(x)$ on $r_i(x)$ for all $i \in \{0\} \cup \mathcal{I}_t$.

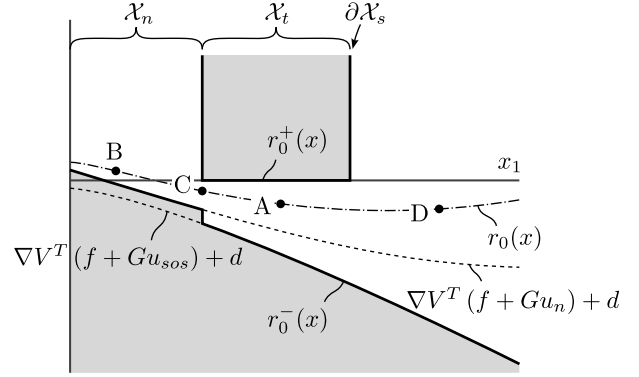


Fig. 5. (Upper and lower bounds on $r_0(x)$): Whereas the upper bound $r_0^+(x)$ is directly given by the finite-time convergence condition in (17), only an estimate of the lower bound $r_0^-(x)$ can be obtained by the solution of the SOS constraints in (36) involving $u_{\text{sos}} := p(x)/s(x)$ and the nominal controller $u_n(x)$.

Example 1: We illustrate a typical design choice for $r_0(x)$ in Figure 5.

For states inside the transitional region $x \in \mathcal{X}_t$ (see point **A** in Figure 5), $r_0(x)$ is required to be smaller than the upper bound $r_0^+(x) = 0$ for (37) to satisfy the finite-time convergence condition in (17). On the other hand, an estimate of the lower bound on $r_0(x)$ can be obtained from the solution $u_{\text{sos}}(x) = p(x)/s(x)$ of the SOS problem in (36). The corresponding lower bound is then given by $r_0^-(x) = \nabla V(x)^T (f(x) + G(x)u_{\text{sos}}(x)) + d(x)$, which is smaller than the upper bound $r_0^+(x) = 0$ within \mathcal{X}_t due to (27b). We wish to emphasize that there may exist more optimal lower bounds on $r_0(x)$; however, the one chosen is certified by the SOS constraints developed in the previous chapter.

For states inside the nominal region $x \in \mathcal{X}_n$ (see point **B** in Figure 5), no upper bound is specified. Hence, by selecting a large $r_0(x)$, we can relax the corresponding constraint of the QCQP in (37). Applying the same approach to other $r_i(x)$ allows us to enlarge the feasible set until $u := u_n(x)$ is a feasible solution for the QCQP, required to satisfy (9). Therefore, we propose the following lower bound: $r_0^-(x) = \nabla V(x)^T (f(x) + G(x)u_n(x)) + d(x)$. By assigning $u := u_n(x)$, the corresponding constraint of the QCQP, expressed as $r_0^-(x) - r_0(x) \leq 0$, is clearly satisfied.

For states on the boundary of the nominal region $x \in \partial \mathcal{X}_n$ (see point **C** in Figure 5), we must ensure compatibility of the lower and upper bounds discussed in the previous paragraphs. More concretely, we need to ensure that $\nabla V(x)^T (f(x) + G(x)u_n(x)) + d(x) \leq 0$ for all $x \in \partial \mathcal{X}_n$. However, this inequality follows directly from inequality (27c).

Finally, for states outside the safe set $x \notin \mathcal{X}_s$ (see point **D** in Figure 5), an upper bound on $r(x)$ is not specified. The lower bound can be chosen as in **A**. It is however important to note that the region can be made attracting with respect to the safe set by the additional requirement of selecting a negative $r(x)$. This can restore the system state to the safe set in scenarios where unexpected system noise or model mismatch cause the

system to deviate from the safe set. ■

Remark 2: In the literature on safety filters, see for example [3], the negative of the allowed reduction of dissipation rate and allowed safety violation are usually specified by class \mathcal{K} functions $\alpha(V(x))$ and $\gamma_i(B_i(x))$:

$$\nabla V(x)^T (f(x) + G(x)u) \leq -\alpha(V(x)), \quad (38a)$$

$$\nabla B_i(x)^T (f(x) + G(x)u) \leq -\gamma_i(B_i(x)) \quad i \in \mathcal{I}_t. \quad (38b)$$

In this case, the class \mathcal{K} functions α and γ_i depend on the value of CLF $V(x)$ and CBFs $B_i(x)$, whereas in the QCQP defined in (37), $r_i(x)$ depend directly on the state x , allowing for more flexibility in choosing the allowed reduction of dissipation rate and safety violation.

From the arguments in Example 1, we derive the following upper and lower bounds on $r_0(x)$:

$$r_0^+(x) := \begin{cases} 0 & \text{if } x \in \mathcal{X}_t \\ \infty & \text{otherwise} \end{cases} \quad (39a)$$

$$r_0^-(x) := \begin{cases} \nabla V(x)^T (f(x) + G(x)u_n(x)) + d(x) & \text{if } x \in \mathcal{X}_n \\ \nabla V(x)^T (f(x) + G(x)u_{\text{sos}}(x)) + d(x) & \text{otherwise} \end{cases} \quad (39b)$$

Applying analogous arguments for the other $r_i(x)$, $i \in \mathcal{I}_t$, the following upper and lower bounds can be derived:

$$r_i^+(x) := \begin{cases} 0 & \text{if } x \in \partial \mathcal{X}_s \cap B_i(x) = 0 \\ \infty & \text{otherwise} \end{cases} \quad (40a)$$

$$r_i^-(x) := \begin{cases} \nabla B_i(x)^T (f(x) + G(x)u_n(x)) & \text{if } x \in \mathcal{X}_n \\ \nabla B_i(x)^T (f(x) + G(x)u_{\text{sos}}(x)) & \text{otherwise} \end{cases} \quad (40b)$$

To establish local Lipschitz-continuity of the safety filter, we need the following assumption.

Assumption 3 (LICQ): The Linear Independence Constraint Qualification (LICQ) is satisfied for the QCQP in (37) across all states x and inputs u , that is, the gradients w.r.t. u of the active inequality constraints in (37) are linearly independent. Equivalently, the rows of $C(x)$ associated with the active inequality constraints are linearly independent.

Remark 3: By extending the QCQP in (37) with a slack variable $\delta \in \mathbb{R}^{t+1}$ as in [19]

$$u_s(x) := \underset{(u, \delta) \in \mathcal{U} \times \mathbb{R}^{t+1}}{\text{argmin}} \quad \|u_n(x) - u\|^2 + \lambda \|\delta\|^2 \\ \text{s.t.} \quad C(x)^T u + b(x) + \delta \leq 0,$$

we automatically satisfy the LICQ property, as demonstrated in [19]. However, the introduction of these slack variables pose the potential risk of compromising safety and finite-time convergence guarantees. That being said, the LICQ assumption is a mild one, it can be met by design, and it generically holds true, i.e., for almost all polynomial coefficients, the Jacobian of a set of polynomials has full rank.

The local Lipschitz-continuity not only preserves existence and uniqueness of solutions (cf. [14][Theorem 3.1]), but can also avoid the resulting feedback controller from chattering, as explained in [20]. The following theorem establishes local

Lipschitz-continuity of the developed QCQP controller. Its proof can be found in the appendix.

Theorem 2: Under Assumption 3, given a smooth CBF $B(x)$ and CLF $V(x)$ as specified in Problem 1, a smooth nominal controller $u_n(x)$, and twice differentiable $r_i(x)$, $i \in \{0\} \cup \mathcal{I}_t$, lower bounded by $r_i^-(x)$, then $u_s(x)$ as defined in (37) is locally Lipschitz-continuous on the safe set \mathcal{X}_s .

VI. ALTERNATING ALGORITHM

The solution of the SOS problem (36) presents a particular challenge due to its bilinearity, i.e., the simultaneous search for CBF $B(x)$, CLF $V(x)$, a rational controller $u_{\text{SOS}}(x)$, and other SOS polynomials introduced by the Positivstellensatz. This bilinearity prevents us from converting the SOS problem directly into a Semi-Definite Program (SDP). Similar to [7], [10], however, we can iteratively alternate between searching over one set of decision variables while keeping the others fixed. Such an alternating algorithm requires a feasible initialization of the decision variables that are kept fixed in the SDP of the first iteration. Therefore, we propose an initialization procedure to find such an initial set of feasible parameters following the presentation of the main algorithm.

A. Main algorithm

To make the main algorithm compatible with the initialization procedure, we introduce an *operating region* that contains the allowable set \mathcal{X}_a :

$$\mathcal{X}_{\text{op}} := \{x \mid f_{\text{op}}(x) \leq 0\} \supseteq \mathcal{X}_a, \quad (41)$$

with scalar polynomial $f_{\text{op}} \in R[x]$. We assume that there exists a constant $\rho_{\Sigma} \in \mathbb{R}$ such that

$$f_{\text{op}}(x) + \rho_{\Sigma} \in \Sigma[x] \quad (42)$$

is an SOS polynomial. This assumption, while not overly restrictive, is important for establishing the feasibility of the SDP in *Part 1* of the initialization procedure, as elaborated in the subsequent subsection.

Remark 4: The operating region \mathcal{X}_{op} can be determined by solving another SOS problem, as condition (42) directly translates to an SOS constraint. By making minor adjustments, it is possible to define the operating region \mathcal{X}_{op} using multiple polynomials, and it could even coincide with the allowable set \mathcal{X}_a . However, in order to reduce computational complexity, we restrict the number of polynomials to one. In cases, where the operating region \mathcal{X}_{op} closely approximates the safe set \mathcal{X}_s , the polynomials $B_i(x)$ in the quadratic modules of the SOS problem in (36) can be omitted, thereby reducing the total number of decision variables. This will reduce computational complexity by introducing slightly more conservative SOS constraints.

The constraint $f_{\text{op}}(x) \leq 0$ defining the operating region \mathcal{X}_{op} is added to the empty set conditions (24) developed in Section IV. From a set-theoretic point of view, adding the constraint $f_{\text{op}}(x) \leq 0$ does not alter the empty set conditions, given that $\mathcal{X}_s \subseteq \mathcal{X}_{\text{op}}$. However, by applying Putinar's P-satz

on the empty set conditions (24) including $f_{\text{op}}(x) \leq 0$, we obtain slightly different SOS constraints for all $i \in \mathcal{I}_t$:

$$-\nabla V^T (sf + Gp) - sd \in \mathbf{M}(V, -B_{\mathcal{I}_t}, -f_{\text{op}}) \quad (43a)$$

$$-\nabla B_i^T (sf + Gp) \in \mathbf{M}(B_i, -B_{\mathcal{I}_t}, -f_{\text{op}}) \quad (43b)$$

$$-\nabla V^T (f + Gu_n) - d \in \mathbf{M}(V, -V, -f_{\text{op}}). \quad (43c)$$

These SOS constraints are used to define the main algorithm.

The main algorithm involves alternating between two SDPs, as described by *Part 1* and *Part 2* below. Given an initial set of feasible parameters, the SDP in *Part 1* is guaranteed to be feasible for each iteration when utilizing the solution from *Part 2*. Likewise, the SDP in *Part 2* is guaranteed to be feasible for each iteration when utilizing the solution from *Part 1*. Furthermore, as shown in [7], the cost of the SDP in *Part 1* encoding the volume of the safe set is non-decreasing over the iterations.

Part 1 - Searching for CBF and CLF: In the first part, we search over CBFs $B_i(x)$ and a CLF $V(x)$ that maximize the volume of the safe set. To make the SDP computationally tractable, we approximate the volume of the safe set by the summation of traces of Q_{B_i} , similar to [6], [21]:

$$\begin{aligned} &\text{find} && V, B_i \in R[x] \\ &\text{hold fixed} && p, s \\ &\text{maximize} && \sum_{i \in \mathcal{I}_t} \text{tr}(Q_{B_i}) \\ &\text{subject to} && (33), (35) \text{ and } (43), \end{aligned}$$

where the Q_{B_i} are derived from the decomposition of the CBF $B_i(x)$ into $B_i(x) = Z_{B_i}(x)^T Q_{B_i} Z_{B_i}(x)$ (cf. (1)).

Part 2 - Searching for a controller: For the second part of the main algorithm, we search over a rational controller $u_{\text{SOS}}(x) = p(x)/s(x)$ that maximizes the SOS constraint margins, denoted by $\Delta_i \in \mathbb{R}$, $i \in \{0\} \cup \mathcal{I}_t$. Only the first two SOS constraints from (43) depend on the rational controller. They are specified with the inclusion of these margins Δ_i as:

$$-\nabla V^T (sf + Gp) - sd + \Delta_0 \in \mathbf{M}(B_i, -B_{\mathcal{I}_t}, -f_{\text{op}}) \quad (44a)$$

$$-\nabla B_i^T (sf + Gp) + \Delta_i \in \mathbf{M}(B_i, -B_{\mathcal{I}_t}, -f_{\text{op}}) \quad (44b)$$

for all $i \in \mathcal{I}_t$. Large values of Δ_i , $i \in \{0\} \cup \mathcal{I}_t$, will increase the set of feasible solution in *Part 1* in the subsequent iterations. The SDP involved in *Part 2* is given by:

$$\begin{aligned} &\text{find} && p \in (\mathbb{R}[x])^m, s \in \Sigma[x], \Delta_i \in \mathbb{R} \\ &\text{hold fixed} && V, B_i \\ &\text{maximize} && \sum_{i \in \{0\} \cup \mathcal{I}_t} \Delta_i \\ &\text{subject to} && (29), (30) \text{ and } (44) \\ &&& s - \epsilon \in \Sigma[x], \Delta_{\min} \leq \Delta_i. \end{aligned} \quad (45)$$

A constant $\epsilon > 0$ assures that $s(x) > 0$. The minimum margin $\Delta_{\min} < 0$ is selected to maintain numerical stability of the algorithm. The main algorithm concludes when the increment in $\sum_{i \in \mathcal{I}_t} \text{tr}(Q_{B_i})$ in *Part 1* does not exceed a predefined minimal threshold.

B. Initialization procedure

The main algorithm, presented in previous subsection, requires an initial set of feasible parameters. Therefore, we present an initialization procedure to find such an initial set.

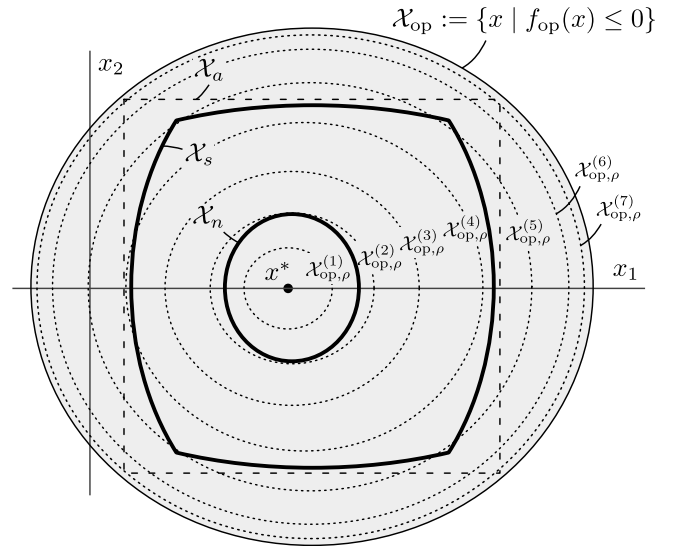


Fig. 6. (Operating region): The initialization procedure produces an initial set of feasible parameters for the main algorithm by iteratively expanding the operating region $\mathcal{X}_{\text{op},\rho}$. The initialization procedure finishes if $\mathcal{X}_{\text{op}} = \mathcal{X}_{\text{op},\rho}^{(k)}$.

Similar to the main algorithm, the initialization procedure involves an alternating between two SDPs, as described by *Part 1* and *Part 2* below. The feasibility of each part is guaranteed by employing the solution of the SDP from the previous iteration. To make sure that the SDP in *Part 1* is feasible in the first iteration, we use a modified operating region (cf. (41))

$$\mathcal{X}_{\text{op},\rho} := \{x \mid f_{\text{op}}(x) + \rho \leq 0\}, \quad (46)$$

with $\rho \geq 0$. By choosing the $\mathcal{X}_{\text{op},\rho}$ initially sufficiently small in volume, i.e., a large $\rho > 0$, we guarantee feasibility of the SDP in *Part 1* for any initial set of parameters, as shown in Lemma 4.

By applying Putinar's P-satz on the modified empty set condition (24) including $f_{\text{op}} + \rho \leq 0$ instead, we derive the following SOS constraints for all $i \in \mathcal{I}_t$:

$$-\nabla V^T (sf + Gp) - sd \in \mathbf{M}(V, -B_{\mathcal{I}_t}, f_{\text{op}} + \rho) \quad (47a)$$

$$-\nabla B_i^T (sf + Gp) \in \mathbf{M}(B_i, -B_{\mathcal{I}_t}, f_{\text{op}} + \rho) \quad (47b)$$

$$-\nabla V^T (f + Gu_n) - d \in \mathbf{M}(V, -V, f_{\text{op}} + \rho). \quad (47c)$$

Part 1 - Searching for CBF and CLF: The first part of the initialization procedure searches over CBF and a CLF that maximize ρ , thereby increasing the volume of $\mathcal{X}_{\text{op},\rho}$ for every iteration (cf. Figure 6). To make sure that $\mathcal{X}_{\text{op},\rho}^{(k)}$ is contained in the operating region, i.e., $\mathcal{X}_{\text{op},\rho}^{(k)} \subseteq \mathcal{X}_{\text{op}}$, we impose the constraint that $0 \leq \rho$. The resulting SDP is expressed as:

$$\begin{aligned} &\text{find} && V, B_i \in R[x], \rho \in \mathbb{R} \\ &\text{hold fixed} && p, s \\ &\text{maximize} && \rho \geq 0 \\ &\text{subject to} && (33), (35) \text{ and } (47). \end{aligned} \quad (48)$$

The next lemma establishes feasibility of the SDP (48) in the first iteration. Its proof can be found in the appendix.

Lemma 4: Assuming that there exist candidates $V(x)$ and $B_i(x)$ that satisfy conditions (33) and (35), then the SDP

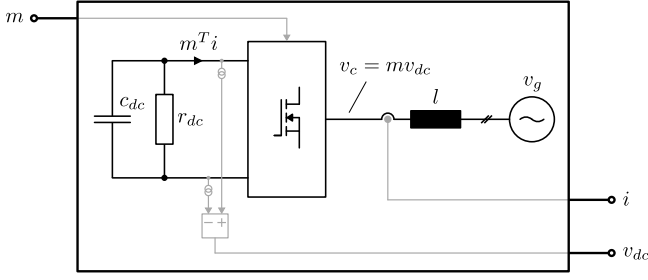


Fig. 7. (Ac/dc converter schematic): The schematic is presented in the (dq) rotating frame, comprising a DC-link, 3-phase bridge, and an ac-line connected to an infinite bus v_g . Assuming the average-value model for the 3-phase bridge, the input $\bar{u} = [m_d \ m_q]^T$ determines the converter voltage v_c as a function of the dc-link voltage v_{dc} . Likewise, the dc-current flowing into the capacitor c_{dc} is given by the input \bar{u} and the ac-line current $i = [i_d \ i_q]^T$. The states consisting of the dc-link voltage v_{dc} and the line-current i are measured.

in (48) is feasible using random initial coefficient values for polynomials $p(x) \in (\mathbb{R}[x])^m$ and $s(x) \in \Sigma[x]$.

Part 2 - Searching for a controller: Similar to the main algorithm, we search over a rational controller $u_{\text{SOS}}(x) = p(x)/s(x)$ that maximizes the SOS constraint margins, denoted by $\Delta_i \in \mathbb{R}$, $i \in \{0\} \cup \mathcal{I}_t$. The corresponding SOS constraints including these margins Δ_i are specified as:

$$-\nabla V^T (sf + Gp) - d + \Delta_0 \in \mathbf{M}(V, -B_{\mathcal{I}_t}, f_{\text{op}} + \rho) \quad (49a)$$

$$-\nabla B_i^T (sf + Gp) + \Delta_i \in \mathbf{M}(B_i, -B_{\mathcal{I}_t}, f_{\text{op}} + \rho), \quad (49b)$$

for all $i \in \mathcal{I}_t$. The resulting SDP is given by:

$$\begin{aligned} &\text{find} && p \in (\mathbb{R}[x])^m, s \in \Sigma[x], \Delta_i \in \mathbb{R} \\ &\text{hold fixed} && V, B_i, \rho \\ &\text{maximize} && \sum_{i \in \{0\} \cup \mathcal{I}_t} \Delta_i \\ &\text{subject to} && (29), (30) \text{ and } (49), \\ &&& s - \epsilon \in \Sigma[x], \Delta_{\min} \leq \Delta_i. \end{aligned}$$

A constant $\epsilon > 0$ assures that $s(x) > 0$. Similar to the SDP (45), the minimum margin $\Delta_{\min} < 0$ is selected to maintain numerical stability of the algorithm. The initialization procedure is considered complete when $\rho = 0$, i.e., $\mathcal{X}_p^{(k)} = \mathcal{X}_{\text{op}}$. At this point, we found an initial set of feasible parameters for the SDP in *Part 1* of the main algorithm.

Remark 5: The initialization procedure can be extended with additional steps where the margins Δ_i are introduced when searching over the controller, or the operational region is expanded – by decreasing ρ – when searching for CBF and CLF. Furthermore, we can introduce additional steps where we optimize only over a subset of the Δ_i 's.

VII. POWER CONVERTER CASE STUDY

The alternating algorithm from Section VI is implemented for a vector field realization of an ac/dc power converter model connected to an infinite bus, as illustrated in Figure 7. A feedback controller that avoids unsafe states is of paramount importance for this application since all electrical variables (e.g. voltages and currents) need to be constrained at all times. For more details about the modelling of power converters, we refer the reader to [22].

The signals are represented in the (dq) rotating frame aligned with the phase $\theta = \omega_n t$ of the grid voltage v_g , where $\omega_n = 2\pi 50$ is the nominal angular frequency in Hz. The signals are given in per-unit representation. The system's dynamics are given as follows:

$$(1/\omega_n)c_{dc}\dot{v}_{dc} = -g_{dc}v_{dc} - i_d m_d - i_q m_q \quad (50a)$$

$$(1/\omega_n)l\dot{i}_d = \omega l i_q + v_{dc} m_d - 1 \quad (50b)$$

$$(1/\omega_n)l\dot{i}_q = -\omega l i_d + v_{dc} m_q, \quad (50c)$$

where $l = 0.01$ is the inductance in p.u. consisting of transformer and line inductance, $c_{dc} = 0.02$ is the dc-link capacitance in p.u., and $g_{dc} := 1/r_{dc} = 0.001$ is the admittance of the DC-link capacitor in p.u. The measured states are denoted by $\bar{x} := [v_{dc} \ i_d \ i_q]^T$, and the input is given by $\bar{u} := [m_d \ m_q]^T$, describing the modulation indices. The objective is to stabilize both the DC-link voltage v_{dc} to 1, and the quadrature current i_q to its reference $i_{q,ref}$, which is assumed to be constant. As a consequence, to meet the steady-state specifications, the direct current i_d is stabilized to $-g_{dc}$. The allowable set of states must adhere to the following inequality constraints:

$$0.2 \leq v_{dc} \leq 1.2, \quad i_d^2 + i_q^2 \leq (1.2)^2. \quad (51)$$

Furthermore, the quadratic input constraint \mathcal{U} is given by

$$m_d^2 + m_q^2 \leq (1.2)^2. \quad (52)$$

The system's equilibrium is characterized by

$$x^* = \begin{bmatrix} 1 \\ -g_{dc} \\ i_{q,ref} \end{bmatrix}, u^* = \begin{bmatrix} 1 - \omega l i_{q,ref} \\ -\omega l g_{dc} \end{bmatrix}.$$

We introduce the error coordinates for the states $x = \bar{x} - x^* = [\tilde{v}_{dc} \ \tilde{i}_d \ \tilde{i}_q]^T$ and the input variables $u = \bar{u} - u^* = [\tilde{m}_d \ \tilde{m}_q]^T$ such that $\dot{x} = 0$ at $x = 0$ and $u = 0$. The system represented in error coordinates is described by system (2) with

$$f(x) = \begin{bmatrix} -0.05\tilde{v}_{dc} - 57.9\tilde{i}_d + 0.00919\tilde{i}_q \\ 1710\tilde{v}_{dc} + 314\tilde{i}_q \\ -0.271\tilde{v}_{dc} - 314\tilde{i}_d \end{bmatrix}$$

$$G(x) = \begin{bmatrix} 0.05 - 57.9\tilde{i}_d & -57.9\tilde{i}_q \\ 1710 + 1710\tilde{v}_{dc} & 0 \\ 0 & 1710 + 1710\tilde{v}_{dc} \end{bmatrix}.$$

We consider a nominal controller that resembles the proportional part of the synchronous rotating frame control structure, as described in [23]:

$$u_n(x) = \begin{bmatrix} 0.1\tilde{v}_{dc} - \tilde{i}_d \\ i_{q,ref} - \tilde{i}_q \end{bmatrix}.$$

In the following subsection, we first consider a single quadrature current reference set to $i_{q,ref} = 0$. Then, we introduce a quadrature current reference as a new state to the dynamical system, with a zero time-derivative, i.e., $\dot{i}_{q,ref} = 0$. For each scenario, we find the CBFs $B_i(x)$ and CLF $V(x)$ (cf. Problem 1) by employing the alternating algorithm in Section VI, and perform simulations including the advanced

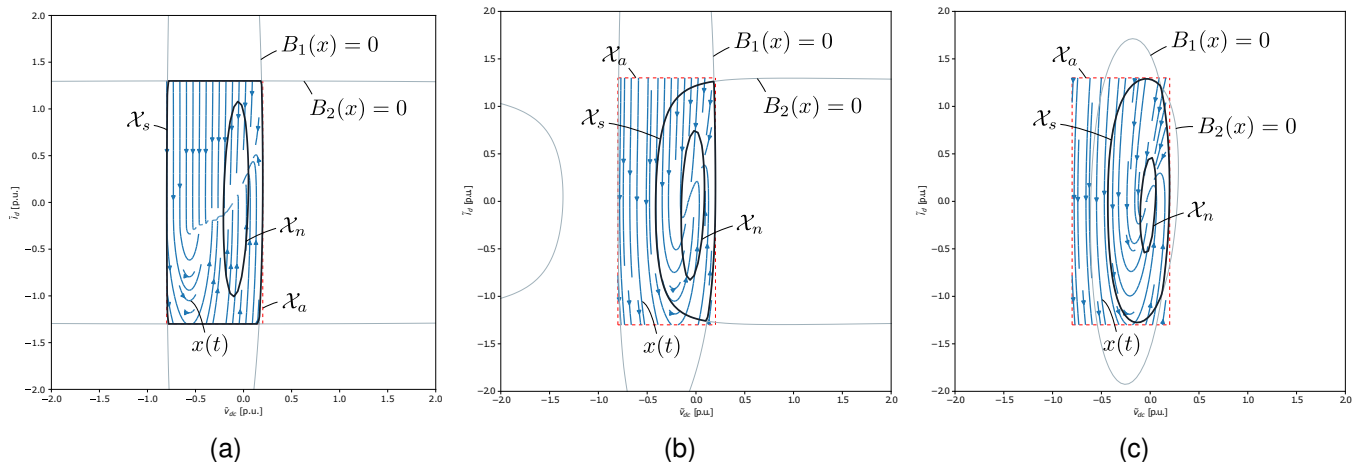


Fig. 8. (Safe set and nominal region): The allowable set \mathcal{X}_a , the safe set \mathcal{X}_s , and the nominal region \mathcal{X}_n projected to the \tilde{v}_{dc} and \tilde{i}_d coordinate are shown for $\tilde{i}_q = i_{q,ref} = 0$. In addition, the zero-level sets of the polynomials $B_1(x)$ and $B_2(x)$ are shown in grey. Three scenarios are shown, where (a) the input action is subjected to no constraints, i.e. $u(x(t)) \in \mathbb{R}^m$, (b) the input action is subjected to a quadratic constraint given by $u(x(t)) \in \mathcal{U} := \{u \mid u^T u \leq 1.3\}$, and (c) $i_{q,ref}$ is integrated as a new state of the dynamical system using the same input constraints. The corresponding vector field $\dot{x} = f(x) + G(x)u_{sos}(x)$ (projected to $(\tilde{v}_{dc}, \tilde{i}_d)$ coordinates) is shown in blue, where $u_{sos}(x) = p(x)/s(x)$ is used to ensure compatibility between the CBF and CLF.

safety filter $u_s(x)$ (cf. Problem 2), and a traditional safety filter implementation. We use `CVXOPT Python` library to solve the SDPs of the alternating algorithm, and to implement the QCQP in (20). This library implements an optimization problem solver based on second-order and positive semidefinite cones. The simulations are performed using the ODE solver from `scipy` with a sampling time of $1 \mu s$.

A. Zero quadrature current reference tracking

In this subsection, we assume a zero quadrature current reference, i.e., $i_{q,ref} = 0$. The allowable set \mathcal{X}_a , as expressed in (15), encoding the state constraints (51), are achieved through the following polynomials:

$$\begin{aligned} w_1(x) &= ((\tilde{v}_{dc} + 0.3)/0.5)^2 + (\tilde{i}_d/20)^2 + (\tilde{i}_q/20)^2 - 1 \\ w_2(x) &= (\tilde{v}_{dc}/20)^2 + (\tilde{i}_d/1.3)^2 + (\tilde{i}_q/1.3)^2 - 1. \end{aligned}$$

The function defining the operating region in (41) is given by:

$$f_{op} = 0.2595\tilde{i}_d^2 + 0.2595\tilde{i}_q^2 + 3.509\tilde{v}_{dc}^2 + 2.105\tilde{v}_{dc} - 1.$$

Figures 8 (a) and (b) illustrates the safe set \mathcal{X}_s and the nominal set \mathcal{X}_n computed by the algorithm both without and with considering inputs constraints. When no input constraints are taken into account, the safe set tightly fits the allowable set \mathcal{X}_a (cf. 8 (a)). However, upon introducing the quadratic inputs constraints in (52), the safe set \mathcal{X}_s becomes noticeably smaller (cf. 8 (b)). The resulting CBFs $B_i(x)$ and CLF $V(x)$ guarantee existence of a safety filter $u_s(x)$, as defined in (20). Table I summarizes both the number of variables associated with the respective SDPs and the number of constraints, derived from the summation of triangular elements within the positive semidefinite matrices. The initialization procedure completed in 10 iterations, where each iteration took around 10 seconds. The main algorithm completed in 20 iterations, where each iteration took around 14 seconds. The degree of the polynomials are summarized in Table II.

TABLE I
SUMMARY OF SDP VARIABLES AND CONSTRAINTS

Scenario		init 1	init 2	main 1	main 2
Fig. 8(a)	Variables	475	187	410	475
	Constraints	5726	4425	5807	5726
Fig. 8(b)	Variables	506	197	441	506
	Constraints	6102	4765	6183	6102
Fig. 8(c)	Variables	1086	357	981	1086
	Constraints	21277	17327	21474	21277

TABLE II
DEGREE OF THE POLYNOMIALS ENCODING THE CLF, CBF, AND THE RATIONAL CONTROLLER

$V(x)$	$B_i(x)$	$p(x)$	$s(x)$
4	4	3	2

Figures 9 and 10 show two simulations, where the safety filter $u_s(x)$ based on the previously computed CLF and CBF is compared to a traditional safety filter $u_{SF}(x)$ using the same CBFs. Following [3], the traditional safety filter $u_{SF}(x)$ is implemented as the following QP:

$$\begin{aligned} \underset{u \in \mathcal{U}}{\operatorname{argmin}} \quad & \|u_n(x) - u\|^2 \\ \text{s.t.} \quad & \nabla B_1(x)(f(x) + G(x)u) + \alpha B_1(x) \leq 0 \\ & \nabla B_2(x)(f(x) + G(x)u) + \alpha B_2(x) \leq 0, \end{aligned} \quad (55)$$

where α is selected to be 10. The variable α determines the allowed safety violation similar to $r_i(x)$, as discussed in Section V. Hence, by increasing the value α , it becomes less likely that the safety filter modifies the nominal control action within the safe set. On the other hand, for a large α , the safety filter becomes more sensitive on system mismatch or measurement noise when approaching the boundary of the safe set. This increased sensitivity can potentially result in closed-loop instabilities.

The simulation in Figure 9 illustrates the effect on including the input constraints into the design of the safety filter

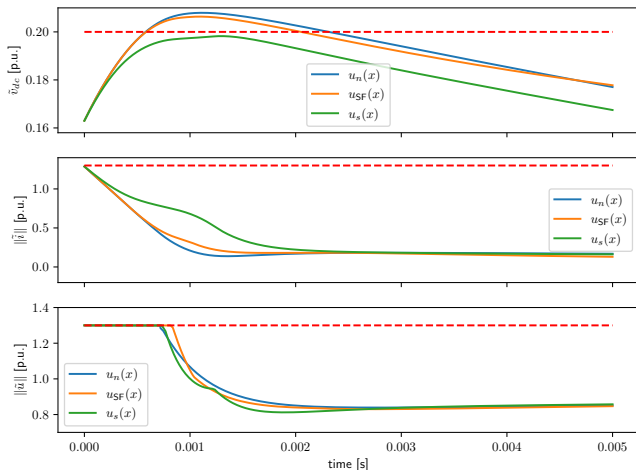


Fig. 9. (Forward invariance of the safe set \mathcal{X}_s): While the advanced safety filter $u_s(x)$, which considers the quadratic input constraints into the design, successfully stays within the state constraints, the nominal controller u_n and traditional safety filter $u_{SF}(x)$ violate the state constraints.

$u_s(x)$. Since the input constraints are incorporated into the design of the CLF and CBFs, as well as the safety filter $u_s(x)$ implementation, it successfully stays within the state constraints for all $t \geq 0$. This is not true for the traditional safety filter $u_{SF}(x)$ that does not consider the input constraints in its implementation. In this case, the norm of the input action $\|u_{SF}(x)\|$ exceeds the input constraint limit of 1.3 p.u. in the beginning of the simulation (cf. Figure 9). To produce a valid input, the input action $u_{SF}(x)$ is projected to the set of feasible input set \mathcal{U} . As a result, the trajectory deviates from its intended path, leading to a violation of the dc-link voltage constraint.

Next, we illustrate the effect of the finite-time convergence property presented in (17). In Figure 10, a simulation is conducted from an initial state located well within the safe set. In this simulation, the safety filter $u_s(x)$ does not modify the nominal control action as the convergence property is satisfied. Conversely, the traditional safety filter provides no guarantee about convergence to the nominal set. Therefore, this safety filter suboptimally modifies the control action, resulting in a much slower convergence.

B. Including current reference tracking

For this subsection, the objective is to stabilize both the DC-link voltage to 1, and the quadrature current to some (not yet a priori pre-specified) quadrature current reference $i_{q,ref}$. To render our design parametric in $i_{q,ref}$, we introduce a new state representing the quadrature current reference. Consequently, we augment the dynamics from (50) with $\dot{i}_{q,ref} = 0$. The corresponding coordinates of the states and inputs are given by $x = [\tilde{v}_{dc} \ \tilde{i}_d \ \tilde{i}_q \ \tilde{i}_{q,ref}]^T$ and $u := [\tilde{m}_d \ \tilde{m}_q]^T$, where $\tilde{i}_{q,ref} = i_{q,ref}$. The allowable set \mathcal{X}_a is chosen through

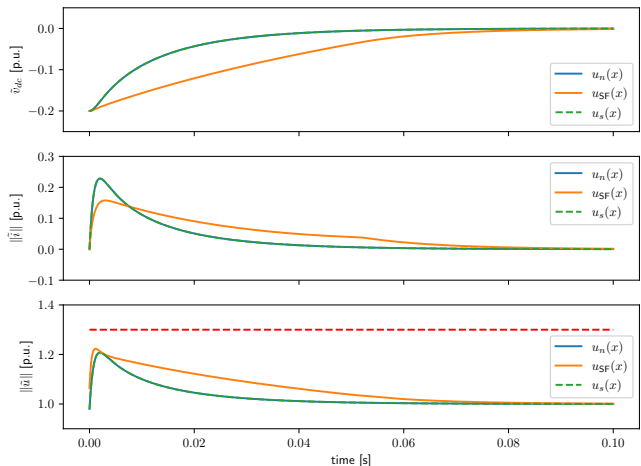


Fig. 10. (Convergence to the nominal region \mathcal{X}_n): While the advanced safety filter $u_s(x)$ essentially overlaps the nominal control u_n , the traditional safety filter $u_{SF}(x)$ suboptimally perturbs the nominal control action, resulting in a much slower convergence.

the following polynomials:

$$w_1(x) = ((\tilde{v}_{dc} + 0.3)/0.5)^2 + (\tilde{i}_d/20)^2 + (\tilde{i}_q/20)^2 + (\tilde{i}_{q,ref}/20)^2 - 1$$

$$w_2(x) = (\tilde{v}_{dc}/20)^2 + (\tilde{i}_d/1.3)^2 + (\tilde{i}_q/1.3)^2 + (\tilde{i}_{q,ref}/20)^2 - 1.$$

The function defining the operating region in (41) is given by:

$$f_{op} = 0.1460\tilde{i}_d^2 + 0.1460\tilde{i}_q^2 + 0.381\tilde{v}_{dc}^2 + 0.2288\tilde{v}_{dc} + 0.8548\tilde{i}_{q,ref} - 1.$$

Correspondingly, a safe set \mathcal{X}_s and the nominal region \mathcal{X}_n can be computed for this 4-dimensional space. By slicing these sets for each $i_{q,ref}$ results in a 3-dimensional safe set and nominal region as defined in the previous subsection. Hence, we can think about it as a family of safe sets parametrized by the variable $i_{q,ref}$. Figure 8(c) illustrates the safe set \mathcal{X}_s and the nominal set \mathcal{X}_n for $i_q = i_{q,ref} = 0$. Table I summarizes the number of variables of the corresponding SDP for each part, as well as the number of constraints. The initialization procedure completed in 51 iterations, where each iteration took around 60 seconds. The main algorithm completed in 20 iterations, where each iteration took around 90 seconds. The degree of the polynomials are summarized in Table II.

The simulation shown in Figure 11 illustrates the reference tracking performance of our safety filter $u_s(x)$ compared to the traditional safety filter $u_{SF}(x)$ introduced in the previous subsection. The safety filter, although slightly perturbing the nominal controller, guarantees finite-time convergence to the nominal set defined for a quadrature current reference $i_{q,ref}$ of 1. However, the traditional safety filter $u_{SF}(x)$ perturbs the nominal control action, leading to a much slower convergence. In general, as we approach the boundary of the safe set by increasing $i_{q,ref}$, the traditional safety filter is more likely to intervene the nominal control action.

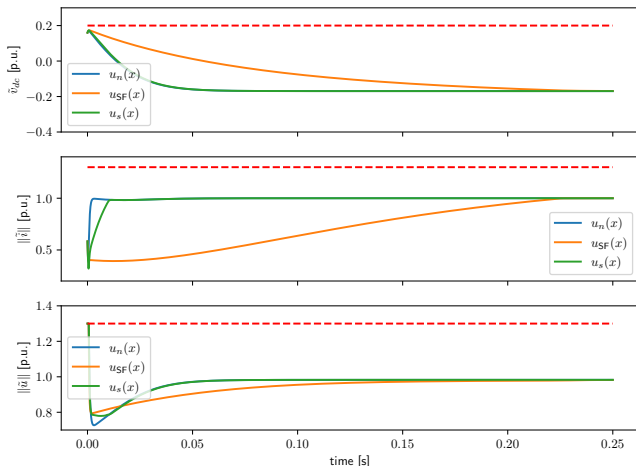


Fig. 11. (Quadrature current reference tracking): The closed-loop simulation demonstrates the finite-time convergence guarantee of the advanced safety filter $u_s(x)$ towards the nominal region \mathcal{X}_n for non-zero quadrature current reference $i_{q,ref} = 1$ p.u. Additionally, the advanced safety filter exhibits a faster convergence to the equilibrium compared to the traditional safety filter $u_{SF}(x)$. The latter is more likely to disturb the nominal control action as the quadrature current reference $i_{q,ref}$ approaches the boundary of the safe set, resulting in a slower convergence.

VIII. CONCLUSION

In this paper, we introduced an advanced safety filter that guarantees safety and preserves the nominal control performance of the nominal controller using CBFs and CLFs. We translated the specifications of this safety filter into an SOS optimization problem, and presented a novel method to encode quadratic input constraints as SOS constraints. We proposed an alternating algorithm to find these CBF and CLF candidates by solving a sequence of SDPs. A concrete realization of the advanced safety filter is provided in form of a QCQP. We tested the advanced safety filter on an ac/dc converter case study, where a nominal controller involving a quadrature current reference is assumed. In a first part, the quadrature current reference is set to zero. In simulations, we then demonstrated the effect on including the quadratic input constraints, as well as the convergence to the nominal region. In a second part, the quadrature current reference is integrated as an additional state of the dynamical system. We demonstrated the capability of the advanced safety filter to maintain the quadrature current tracking behavior of the nominal controller.

Computing global guarantees such as the safe set of a dynamical system is a very powerful tool. However, finding these guarantees is computationally difficult and scales poorly with the number of states and the degrees of the polynomials. We therefore see much potential in improving the alternating algorithm, or in relaxing the CBF and CLF conditions and only compute approximate global guarantees. Furthermore, the safety filter based on online optimization could potentially be enhanced by Model Predictive Control (MPC) methods, enabling a contingency strategy in situations where unexpected system noise deviate the system from the safe set.

IX. APPENDIX

A. Proof of Lemma 1

Because the safe set \mathcal{X}_s is compact and forward invariant, and the closed-loop dynamical system $\dot{x} = f(x) + G(x)u_s(x)$ is Lipschitz-continuous, there exists a unique trajectory $x(t)$ for all $x(0) \in \mathcal{X}_s$ and $t > 0$. The finite-time convergence property in (17) with $u := u_s(x)$ can be written without dissipation rate as $\forall x \in \partial X_n$:

$$\nabla V(x)^T (f(x) + G(x)u_s(x)) \leq 0. \quad (56)$$

Using the tangent cone $T_{\mathcal{X}_n}(x) = \{z \mid \nabla V(x)^T z \leq 0\}$, the condition (56) can be formulated as $\forall x \in \partial X_n$:

$$f(x) + G(x)u_s(x) \in \mathcal{T}_{\mathcal{X}_n}(x).$$

Hence, according to [17, Nagumo's Theorem 4.7], \mathcal{X}_n is forward invariant. This proves that for all $x(0) \in \mathcal{X}_n$, we can choose $T = 0$. It remains to show that for all other initial states, i.e., $x(0) \in \mathcal{X}_t$, there exists $T \geq 0$ such that $x(T) \in \mathcal{X}_n$, or equivalently $V(x(T)) \leq 0$.

As $\mathcal{X}_t \subseteq \mathcal{X}_s$ is compact (cf. Assumption 1) and the dissipative rate $d(x)$ defined in (18) is assumed to be strictly positive and Lipschitz-continuous on \mathcal{X}_t , the following minimum exists: $l = \min_{x \in \mathcal{X}_t} \lambda(x) (V(x) + V_0) > 0$. Therefore, the scalar function $V(x(t))$ strictly decreases over time for all $x(0) \in \mathcal{X}_t$ due to the finite-time convergence condition in (17): $\dot{V} = \nabla V(x)^T (f(x) + G(x)u_s(x)) \leq -l < 0$. Within \mathcal{X}_t , $V(x(t))$ is then upper bounded by: $V(x(t)) \leq V(x(0)) - lt$. Therefore, there exists some $T \leq V(x(0))/l$ such that $V(x(T)) \leq 0$.

B. Derivation of the SOS constraints (25)

The objective of this section is to convert the empty-set condition (24b) into the SOS constraint given in (25b). The derivation of (25a) and (25c) is analogous. Applying Putinar's P-satz to (24b) yields the SOS constraint

$$-\nabla V^T f - d \in \mathbf{M}(\nabla V^T G, -\nabla V^T G, V, -B_{\mathcal{I}_t}).$$

By utilizing the definition of a quadratic module in (4), we can express this SOS constraint by the condition that there exist two SOS polynomials $p_{0,1}, p_{0,2} \in (\Sigma[x])^m$ such that

$$-\nabla V^T (f + G(p_{0,1} - p_{0,2})) - d \in \mathbf{M}(V, -B_{\mathcal{I}_t}).$$

By exploiting the fact that the set of SOS polynomials, when combined with the set of negative SOS polynomials, spans the entire set of polynomials (i.e., $\Sigma[x] - \Sigma[x] = R[x]$), we can reformulate the SOS constraint as the condition that there exists a polynomial $p_0 \in (R[x])^m$ such that

$$-\nabla V^T (f + Gp_0) - d \in \mathbf{M}(V, -B_{\mathcal{I}_t}).$$

Finally, we introduce an additional SOS polynomial $s_0(x)$ (cf. (7)) and rewrite the SOS constraint as the condition that there exists $s_0 \in \Sigma[x], p_0 \in (R[x])^m$ such that

$$-\nabla V^T (s_0 f + Gp_0) - s_0 d \in \mathbf{M}(V, -B_{\mathcal{I}_t}).$$

The introduction of the polynomial $s_0(x)$ increases the set of feasible solutions when truncating the degrees of the involved polynomials, as described in Section II-B.

C. Proof of Lemma 2

By dividing (27a) and (27b) by $s(x) > 0$, we obtain

$$\nabla B_i^T (f + Gu_{\text{SOS}}) + \frac{\gamma_{0,i}}{s} B_i - \frac{\gamma_{1,i}^T}{s} B_{\mathcal{I}_t} \leq 0 \quad (57a)$$

$$\nabla V^T (f + Gu_{\text{SOS}}) + d + \frac{\gamma_{0,0}}{s} V - \frac{\gamma_{1,0}^T}{s} B_{\mathcal{I}_t} \leq 0, \quad (57b)$$

where $u_{\text{SOS}}(x) = p(x)/s(x)$.

From (57a), by using the fact that $\gamma_{1,i}(x) \geq 0$, $s(x) > 0$, and $B_i(x) = 0$ and $B_{\mathcal{I}_t}(x) \leq 0$ on $\partial\mathcal{X}_s$, we infer, for each $i \in \mathcal{I}_t$, that for all $x \in \partial\mathcal{X}_s$ there exists $u := u_{\text{SOS}}(x)$ such that $\nabla B_i^T (f + Gu_{\text{SOS}}) \leq 0$ whenever $B_i(x) = 0$. Or, equivalently, for all $x \in \partial\mathcal{X}_s$ there exists $u := u_{\text{SOS}}(x)$ such that $\nabla B_i^T (f + Gu) \leq 0$ for all $i \in \text{Act}(x)$, as defined in (14). This proves the forward invariance condition in (13) using the definition of the tangent cone under Assumption 2.

From (57b), by using the fact that $\gamma_{0,0}(x) \geq 0$, $\gamma_{1,0}(x) \geq 0$, $s(x) > 0$, and $V(x) \geq 0$ and $B_{\mathcal{I}_t}(x) \leq 0$ on \mathcal{X}_t , we deduce that for all $x \in \mathcal{X}_t$ there exists $u := u_{\text{SOS}}(x)$ such that $\nabla V^T (f + Gu) + \lambda(V - V_0) \leq 0$. This proves the finite-time convergence condition (17).

Finally, from (27c), by using the fact that $V(x) = 0$ on $\partial\mathcal{X}_n$, we deduce that the inequality $\nabla V^T (f + Gu_n) \leq 0$ holds for all $x \in \partial\mathcal{X}_n$. This proves the forward invariance on \mathcal{X}_n condition in (19).

D. Proof of Lemma 3

We use the definition of a quadratic module in (4), to rewrite the SOS constraint in (29) as $\forall x \in \mathbb{R}^n, \exists \gamma_u \in (\Sigma[x])^t$:

$$-a_i u_{\text{SOS}}(x) + b_i + \frac{\gamma_u(x)^T}{s(x)} B_{\mathcal{I}_t}(x) \geq 0$$

for $i \in \mathcal{I}_t$, and $u_{\text{SOS}}(x) = p(x)/s(x)$. Since the $\gamma_u(x) \geq 0$, $s(x) > 0$, and $B_{\mathcal{I}_t}(x) \leq 0$ on \mathcal{X}_s , we deduce, for all $i \in \mathcal{I}_t$, $-a_i u_{\text{SOS}}(x) + b_i \geq 0$ on \mathcal{X}_s . This concludes the first part of the proof.

By substituting the variable v in (31) with $u - u_0$, we can reformulate the SOS constraints by using the definition of a quadratic module as $\forall x \in \mathbb{R}^n, \exists \gamma_{u,1} \in \Sigma[x, u], \gamma_{u,2} \in (\Sigma[x, u])^t$:

$$\begin{aligned} & -((u - u_0)^T Q_u (u_{\text{SOS}}(x) - u_0) - u_{\text{max}}^2) \\ & + \frac{\gamma_{u,1}(x, u)}{s(x)} f_u(x, u - u_0) + \frac{\gamma_{u,2}(x, u)^T}{s(x)} B_{\mathcal{I}_t} \geq 0, \end{aligned} \quad (58)$$

where $x \in \mathbb{R}^n$ and $u \in \mathbb{R}^m$ are the variables of the polynomial expressions. Because of its positive semi-definiteness, Q_u can be decomposed into $Q_u = B_u^T B_u$. Furthermore, since $\gamma_{u,1}(x, u) \geq 0$, $\gamma_{u,2}(x, u) \geq 0$, $s(x) > 0$, $B_{\mathcal{I}_t}(x) \leq 0$ on \mathcal{X}_s , and $f_u(x, u - u_0) \leq 0$ on \mathcal{U} , condition (58) can be reformulated as $\forall x \in \mathcal{X}_s, \forall u \in \mathcal{U}$:

$$(u - u_0)^T B_u^T B_u (u_{\text{SOS}}(x) - u_0) \leq u_{\text{max}}^2. \quad (59)$$

For any $x \in \{x \in \mathcal{X}_s \mid B_u(u_{\text{SOS}}(x) - u_0) = 0\}$, we have $(u_{\text{SOS}}(x) - u_0)^T B_u^T B_u (u_{\text{SOS}}(x) - u_0) = 0 \leq u_{\text{max}}^2$. Hence, $u_{\text{SOS}}(x) \in \mathcal{U}$.

For any other safe state, that is $x \in \{x \in \mathcal{X}_s \mid B_u(u_{\text{SOS}}(x) - u_0) \neq 0\}$, there exists a unique $\lambda > 0$ such that

$$(B_u \lambda (u_{\text{SOS}}(x) - u_0))^T (B_u \lambda (u_{\text{SOS}}(x) - u_0)) = u_{\text{max}}^2. \quad (60)$$

Additionally, substituting u by $\lambda(u_{\text{SOS}}(x) - u_0) + u_0$ in condition (59) yields the condition that $\forall x \in \mathcal{X}_s$:

$$\lambda (B_u (u_{\text{SOS}}(x) - u_0))^T (B_u (u_{\text{SOS}}(x) - u_0)) \leq u_{\text{max}}^2. \quad (61)$$

By comparing (60) and (61), we conclude that λ must be greater than 1. As a consequence, $(B_u (u_{\text{SOS}}(x) - u_0))^T (B_u (u_{\text{SOS}}(x) - u_0)) \leq u_{\text{max}}^2$ holds for all $x \in \mathcal{X}_s$. This concludes that $u_{\text{SOS}}(x) \in \mathcal{U}$ for all $x \in \mathcal{X}_s$.

E. Proof of Theorem 2

Consider the optimization problem

$$\begin{aligned} \min_u \quad & f(u, x) \\ \text{s.t.} \quad & g(u, x) \leq 0, \end{aligned} \quad (62)$$

and a point $x^* \in \mathbb{R}^n$. We say $(u_s(x^*), \lambda(x^*))$ is a *regular minimizer* if the LICQ is satisfied at $u_s(x^*)$, and $(u_s(x^*), \lambda(x^*))$ satisfies the KKT condition and the strong second order sufficient condition (SSOSC). The point (u, λ) satisfies the SSOSC if Hessian matrix of the Lagrangian of (62) is positive definite at this point. According to [24, Theorem 2.3.3], there exists a locally Lipschitz continuous map $u_s(x)$ around a neighborhood of x^* such that $u_s(x) \in \mathbb{R}^m$ is a minimizer for the non-linear optimization problem (62), if f and g are twice continuously differentiable in (u, x) , and $u_s(x^*)$ is a regular minimizer with multiplier $\lambda(x^*)$. In what follows, we establish these conditions for the QCQP in (37).

LICQ property under Assumption 3 asserts that for any solution of the QCQP $u_s(x^*)$, there exists a unique λ^* that satisfies the KKT condition at $(u_s(x^*), \lambda^*)$. Next, we show that the SSOSC holds for any choice of λ^* , specifically λ^* that satisfies the KKT condition. Consider the Lagrangian of the QCQP for either linear or quadratic input constraints:

$$\begin{aligned} L(u, \lambda) = & u^T u + 2u_n(x)u + u_n(x)^T u_n(x) \\ & + \lambda_1^T (C(x)u + b(x)) \\ & + \lambda_2^T (u^T Q_u u - u_{\text{max}}^2) + \lambda_3^T (Au - b) \end{aligned}$$

Then the inequality $v^T \nabla_{uu}^2 L(u, \lambda) v = v^T v + \lambda_2 v^T Q_u v > 0$ for all $v \in \mathbb{R}^m$. This proves that any solution of the QCQP $u_s(x^*)$ satisfies the SSOSC with the corresponding λ^* . Furthermore, a solution of the QCQP $u_s(x)$ exists for all x due to the lower bound on $r_i(x)$, $i \in \mathcal{I}_t$, as explained in Section V, consequently establishing the local Lipschitz continuity of $u_s(x)$.

F. Proof of Lemma 4

By utilizing the definition of a quadratic module in (4), the conditions in (47) can be formulated as the existence of $\gamma_{0,i}, \gamma_n \in R[x]$, $\gamma_{0,0}, \gamma_{\text{op},0}, \gamma_{\text{op},i}, \gamma_{\text{op},n} \in \Sigma[x]$, and $\gamma_{1,i}, \gamma_{1,0} \in (\Sigma[x])^t$ such that

$$g_i + \gamma_{\text{op},i}(f_{\text{op}} + \rho) \in \Sigma[x] \quad (63a)$$

$$g_0 + \gamma_{\text{op},0}(f_{\text{op}} + \rho) \in \Sigma[x] \quad (63b)$$

$$g_n + \gamma_{\text{op},n}(f_{\text{op}} + \rho) \in \Sigma[x], \quad (63c)$$

with polynomials

- $q_i := -\nabla B_i^T (sf + Gp) - \gamma_{0,i} B_i + \gamma_{1,i}^T B_{\mathcal{I}_t}$
- $q_0 := -\nabla V^T (sf + Gp) - sd - \gamma_{0,0} V + \gamma_{1,0}^T B_{\mathcal{I}_t}$
- $q_n := -\nabla V^T (f + Gu_n) - d + \gamma_n V$.

First, we show that for any polynomial $q \in R[x]$, we can find $\gamma_{\text{op}} \in \Sigma[x]$ and $\rho \in \mathbb{R}$ such that

$$q(x) + \gamma_{\text{op}}(x)(f_{\text{op}}(x) + \rho) \in \Sigma[x]. \quad (64)$$

To show this, we select an SOS polynomial $\gamma_{\text{op}} \in \Sigma[x]$ sufficiently large such that $q(x) + \gamma_{\text{op}}(x) \in \Sigma[x]$. This is always possible since starting from the decomposition $q(x) = Z(x)^T Q_f Z(x)$ (cf. (1)), we can select $\gamma_{\text{op}}(x) = \nu Z(x)^T Z(x)$, with arbitrary large $\nu > 0$, such that $Q_f + \nu I \succ 0$. Second, by utilizing the assumption on ρ_{Σ} (cf. (42)), choose $\rho := \rho_{\Sigma} + 1$ such that $q(x) + \gamma_{\text{op}}(x) + \gamma_{\text{op}}(x)(\rho(x) + \rho_{\Sigma}) \in \Sigma[x]$. Hence, any $\rho \geq \rho_{\Sigma} + 1$ renders (64) an SOS polynomial.

In this way, we can find ρ for each SOS constraint in (63), and denote them by $\rho_0, \rho_i, \rho_n \in \mathbb{R}$. By selecting $\rho := \max(\rho_0, \rho_i, \rho_n)$, all SOS constraints in (63) hold simultaneously. Hence, the SOS problem (48) is feasible for any initialization of $q_0(x)$, $q_i(x)$, $i \in \mathcal{I}_t$, and $q_n(x)$.

REFERENCES

- [1] K.P. Wabersich, A.J. Taylor, J.J. Choi, K. Sreenath, C.J. Tomlin, A.D. Ames, and M.N. Zeilinger. Data-driven safety filters: Hamilton-jacobi reachability, control barrier functions, and predictive methods for uncertain systems. *IEEE Control Systems Magazine*, 43(5):137–177, 2023.
- [2] M.Z. Romdlony and B. Jayawardhana. Uniting control Lyapunov and control barrier functions. In *53rd IEEE Conference on Decision and Control*, pages 2293–2298. IEEE, 2014.
- [3] A.D. Ames, S. Coogan, M. Egerstedt, G. Notomista, K. Sreenath, and P. Tabuada. Control barrier functions: Theory and applications. In *2019 18th European control conference (ECC)*, pages 3420–3431. IEEE, 2019.
- [4] A.D. Ames, J.W. Grizzle, and P. Tabuada. Control barrier function based quadratic programs with application to adaptive cruise control. In *53rd IEEE Conference on Decision and Control*, pages 6271–6278. IEEE, 2014.
- [5] A. Clark. Verification and synthesis of control barrier functions. In *2021 60th IEEE Conference on Decision and Control (CDC)*, pages 6105–6112. IEEE, 2021.
- [6] L. Wang, D. Han, and M. Egerstedt. Permissive barrier certificates for safe stabilization using sum-of-squares. In *2018 annual American control conference (ACC)*, pages 585–590. IEEE, 2018.
- [7] M. Schneeberger, F. Dörfler, and S. Mastellone. Sos construction of compatible control Lyapunov and barrier functions. *IFAC-PapersOnLine*, 56(2):10428–10434, 2023. 22nd IFAC World Congress.
- [8] H. Wang, K. Margellos, and A. Papachristodoulou. Safety verification and controller synthesis for systems with input constraints. *IFAC-PapersOnLine*, 56(2):1698–1703, 2023.
- [9] H. Dai and F. Permenter. Convex synthesis and verification of control-Lyapunov and barrier functions with input constraints. In *2023 American Control Conference (ACC)*, pages 4116–4123. IEEE, 2023.
- [10] W. Tan and A. Packard. Searching for control Lyapunov functions using sums of squares programming. *sibi*, 1(1), 2004.
- [11] P. Zhao, R. Ghabcheloo, Y. Cheng, H. Abdi, and N. Hovakimyan. Convex synthesis of control barrier functions under input constraints. *IEEE Control Systems Letters*, 2023.
- [12] A. Isaly, M. Ghanbarpour, R.G. Sanfelice, and W.E. Dixon. On the feasibility and continuity of feedback controllers defined by multiple control barrier functions for constrained differential inclusions. In *2022 American Control Conference (ACC)*, pages 5160–5165. IEEE, 2022.
- [13] G. Valmorbida and J. Anderson. Region of attraction estimation using invariant sets and rational Lyapunov functions. *Automatica*, 75:37–45, 2017.
- [14] H.K. Khalil. *Nonlinear Systems*. Pearson Education. Prentice Hall, 2002.
- [15] P. Wieland and F. Allgöwer. Constructive safety using control barrier functions. *IFAC Proceedings Volumes*, 40(12):462–467, 2007.
- [16] M. Laurent. Sums of squares, moment matrices and optimization over polynomials. *Emerging applications of algebraic geometry*, pages 157–270, 2009.
- [17] F. Blanchini. Set invariance in control. *Automatica*, 35(11):1747–1767, 1999.
- [18] M. Krstic. Inverse optimal safety filters. *IEEE Transactions on Automatic Control*, 2023.
- [19] A.D. Ames, X. Xu, J. W. Grizzle, and P. Tabuada. Control barrier function based quadratic programs for safety critical systems. *IEEE Transactions on Automatic Control*, 62(8):3861–3876, 2016.
- [20] B. Morris, M.J. Powell, and A.D. Ames. Sufficient conditions for the lipschitz continuity of qp-based multi-objective control of humanoid robots. In *52nd IEEE Conference on Decision and Control*, pages 2920–2926. IEEE, 2013.
- [21] S. Kundu, S. Geng, S.P. Nandanoori, I. A. Hiskens, and K. Kalsi. Distributed barrier certificates for safe operation of inverter-based microgrids. pages 1042–1047, 2019.
- [22] N. Mohan, T. M. Undeland, and W.P. Robbins. *Power electronics: converters, applications, and design*. John wiley & sons, 2003.
- [23] F. Blaabjerg, R. Teodorescu, M. Liserre, and A.V. Timbus. Overview of control and grid synchronization for distributed power generation systems. *IEEE Transactions on industrial electronics*, 53(5):1398–1409, 2006.
- [24] K. Jittorntrum. *Sequential algorithms in nonlinear programming*. The Australian National University (Australia), 1978.